

**An-Najah National University
Faculty of Graduate Studies**

Electrochromic Properties of Sol-gel NiO – based films

**By
Atheer Yousef Saleh Abu-Yaqoub**

**Supervisors
Dr. Iyad Saadeddin
Co-Supervisor
Prof. Hikmat Hilal**

**This Thesis is Submitted in Partial Fulfillment of the Requirements
for the Degree of Master of Science in Physics, Faculty of Graduate
Studies, An-Najah National University, Nablus, Palestine.**

2012

Electrochromic Properties of Sol-gel NiO – based films

**By
Atheer Yousef Saleh Abu-Yaqoub**

This thesis was defended successfully on 15/3/2012, and approved by:

Defense Committee Members

Signature

1. Dr. Iyad Saadeddin / Supervisor

.....

2. Prof. Hikmat Hilal / Co-Supervisor

.....

3. Prof. Atef Qasrawi / External Examiner

.....

4. Prof. Ghassan Safareny / Internal Examiner

.....

Dedication

To my husband Amjad , my children

Kareem & Obada

To my father,mother,sisters& brothers espicially

Taha & Mohamed

To those who are looking forward for more knowledge.....

Acknowledgments

The author wishes to express her sincere appreciation to her supervisors Dr. Iyad Saadeddin & Professor Hikmat S. Hilal and for their guidance, help and their moral support throughout research work and writing up.

The author would like to thank Dr. Ahed Zyoud for his help and encouragement throughout research work. Technical help from Chemistry Department Laboratory staff at An-Najah N. University is acknowledged.

Thanks are extended to Dr. DaeHoon Park, (Dansuk, Korea) for help with SEM and XRD measurements. Thanks are also due to Dr. Guy Campet (ICMCB, Bordeaux University, France) and his group for allowing us to use laboratory and equipment. Financial support for this project from Al-Maqdisi program is acknowledged.

I wish to express my appreciation to the patience and encouragements given to me by my family.

Atheer

الإقرار

أنا الموقعة أدناه مقدم الرسالة التي تحمل عنوان

Electrochromic Properties of Sol-gel NiO – based films

التلوين الكهربائي لأفلام NiO المحضرة بطريقة السول – جل

أقر بان ما اشتملت عليه هذه الرسالة إنما هو نتاج جهدي الخاص ، باستثناء ما تمت الإشارة إليه حيثما ورد، وان هذه الرسالة ككل من أو جزء منها لم يقدم من قبل لنيل أية درجة أو بحث علمي أو بحثي لدى أية مؤسسة تعليمية أو بحثية أخرى .

Declaration

The work provided in this thesis, unless otherwise referenced, is the researcher's own work, and has not been submitted elsewhere for any other degree or qualification.

Student's name:

اسم الطالبة:

Signature:

التوقيع:

Date:

التاريخ:

List of Contents

No.	Contents	Page
	Dedication	iii
	Acknowledgements	iv
	Declaration	v
	List of Contents	vi
	List of Tables	viii
	List of Figures	ix
	Abstract	Xiii
	Chapter 1: Introduction	1
1.1	Objectives	2
1.2	Why NiO based thin films ?	3
1.3	Hypothesis	3
1.4	Previous Studies	3
	Chapter 2: Fundamentals and theoretical background	7
2.1	Chromism	8
2.2	Electrochromism	9
2.2.1	Operation & applications of electrochromism devices	9
2.2.2	Materials used in ECDs	12
2.2.3	Types of electrochromic devices	16
2.2.4	Electrochromic device features	17
2.2.5	Benefits with electrochromic windows	19
2.3	Background on nickel compounds	19
2.3.1	Nickle & nickel compounds	19
2.3.2	Nickle(II) oxide, NiO	20
2.3.3	Nickel hydroxide	21
2.3.4	Nickel oxy hydroxide, NiOOH	22
2.3.5	Coloration mechanism of nickel oxide-based thin films	22
2.4	Optical properties: film thickness	24
2.5	Deposition techniques of NiO-based thin films	27
2.5.1	Physical Techniques	27
2.5.2	Chemical techniques	30
2.5.3	Sol-gel process	35
	Chapter 3: Experimental Work	36
3.1	Materials & film preparation	37
3.1.1	Chemicals & solvents	37
3.1.2	Substrate Cleaning Process	37
3.1.3	Preparation of NiO based films	38
3.2	Measurements	42
3.2.1	Cyclic voltammetry	42
3.2.2	Transmittance	43

No.	Contents	Page
3.2.3	Photoluminescence measurements	44
3.2.4	X-Ray Diffraction(XRD)	44
3.2.5	Scanning ElectronMicroscopy(SEM)	45
	Chapter 4: Results & Discussion	47
4.1	Nickel oxide doped with Titanium (NiO:Ti) thin films	48
4.1.1	Cyclic Voltammetry (CV)	49
4.1.2	Optical properties	56
4.1.3	Structural properties	63
4.1.4	Conclusion	67
4.2	Nickel oxide co-doped with Ti and Sn thin films	67
4.2.1	Cyclic Voltammetry (CV):	68
4.2.2	Optical properties	74
4.2.3	Conclusion	84
	Suggestions for Further Works	86
	References	87
	الملخص	ب

List of Tables

No.	Table	Page
Table (2.1)	Some Solid ion-conducting electrolytes for use in ECDs	14
Table (2.2)	Properties of the most studied electrochromic inorganic materials	15
Table (3.1)	list of intended composition, nickel (II) acetate mass, and Ti-isopropoxide mass used in the sol-gel preparation. All sol-gel solutions were prepared in ethanol total volume of 40 ml.	40
Table (3.2)	list of intended composition, Ti-isopropoxide mass, and tin (II) chloride mass used in the sol-gel preparation. All sol-gel solutions contain 3.73 gm of Nickel acetate and they were prepared in ethanol total volume of 40 ml.	41
Table (4.1)	calculated Q_a , Q_c and Q_a/Q_c for cycles 1, 10, 20, and 30 of NiO doped with different molar concentration of Ti.	55
Table (4.2)	contrast ration (T_b/T_c) and coloration efficiency (CE) for cycle 30 of NiO films doped with different molar concentration of Ti.	60
Table (4.3)	calculated Q_a , Q_c and Q_a/Q_c for cycles 1, 10, 20, and 30 of NiO doped with different molar concentrations of Ti and Sn	73
Table (4.4)	calculated contrast ration (T_b/T_c) and coloration efficiency (CE) for cycle 30 of NiO:Ti films doped with different molar concentration of Sn. NiO:Ti _{0.25} is presented here for comparison.	79
Table (4.5)	calculated film thickness for different deposited films on FTO/Glass	82

List of Figure

No.	Figure	Page
Fig. (2.1)	Basic design of an electrochromic device, indicating transport of positive ions under the action of an electric field	9
Fig. (2.2)	Various applications for ECD	11
Fig. (2.3)	ECWs with illustration of visible light and solar haet	12
Fig. (2.4)	Three different types of electrochromic devices (ECDs): (a) solution type, (b) hybrid type, and (c) battery-like type.	17
Fig. (2.5)	Illustration of α -Ni(OH) ₂ and β -Ni(OH) ₂ phases	21
Fig. (2.6)	Illustration of β -NiOOH and γ -NiOOH phases	22
Fig. (2.7)	Schematic diagram for NiO under chemical and electrochemical reaction.	23
Fig. (2.8)	The general reaction scheme proposed by Bode <i>et al</i>	24
Fig. (2.9)	System made of an absorbing thin film on a thick finite transparent substrate	25
Fig. (2.10)	Typical transmission spectrum for a uniform TCO thin film.	25
Fig. (2.11)	Schematic presentation of Principles of the RF magnetron sputtering	28
Fig. (2.12)	A schematic shows the electron beam evaporation technique	29
Fig. (2.13)	A typical configuration of a PLD deposition chamber.	30
Fig. (2.14)	Experimental arrangement for film growth in ECD.	31
Fig. (2.15)	Experimental setup for the chemical bath.	32
Fig. (2.16)	A spin coating process: applying the solution onto the substrate, rotating the substrate and drying. Repeating this process leads to multilayer structure.	33
Fig. (2.17)	Schematic shows the stages of the dip coating process	34
Fig. (2.18)	Schematic representation of sol-gel process to synthesize thin films, nanomaterials and ceramics.	35
Fig. (3.1)	Steps of NiO-based films deposition by dip coating process.	39
Fig. (3.2)	A schematic shows one compartment three electrodes electrochemical cell	42

No.	Figure	Page
Fig (4.1)	Cyclic voltammetry measurements for cycles no 1,10, 20, and 30 for NiO:Ti with different Ti molar concentrations: a) NiO, b) Ni _{0.95} Ti _{0.05} O, c)Ni _{0.9} Ti _{0.1} O, d) Ni _{0.85} Ti _{0.15} O, e) Ni _{0.8} Ti _{0.2} O, f) Ni _{0.75} Ti _{0.25} O, and g) Ni _{0.7} Ti _{0.3} O.	51
Fig. (4.2)	Current density with time for cycles no 1,10, 20, and 30 for NiO:Ti with different Ti molar concentrations: a) NiO, b) Ni _{0.95} Ti _{0.05} O, c)Ni _{0.9} Ti _{0.1} O, d) Ni _{0.85} Ti _{0.15} O, e) Ni _{0.8} Ti _{0.2} O, f) Ni _{0.75} Ti _{0.25} O, and g) Ni _{0.7} Ti _{0.3} O.	53
Fig. (4.3)	Visible range Transparency (T) spectra for glass and FTO/glass substrate; air is set as a reference.	58
Fig. (4.4)	Coloration and bleaching transparency (T) spectra, during CV measurements (cycles 29 & 30), for double layer NiO:Ti with different Ti molar concentrations.	58
Fig. (4.5)	Transparency and current evolution during CV measurement for NiO:Ti _{0.25} layer. (→) indicates the current evolution and (- - - >) indicates corresponding Transparency evolution.	59
Fig. (4.6)	Photoluminescence spectra for glass and NiO:Ti/glass	62
Fig. (4.7)	Scanning for PL excitation wavelengths.	63
Fig. (4.8)	XRD pattern for NiO:Ti with different Ti molar concentration.	64
Fig. (4.9)	Prolong time XRD pattern for NiO:Ti with different Ti molar concentration.	65
Fig. (4.10)	FE-SEM for NiO:Ti films with Ti molar concentration a) 10% and b) 20%.	66
Fig (4.11)	Cyclic voltammetry measurements for cycles no 1, 10, 20, and 30 for Ni _{0.75} Ti _{0.25-y} Sn _y (NiO:Ti:Sn) with y values a) 0.01 b) 0.02 c) 0.03 d) 0.04 e) 0.05 f) 0.15	71
Fig. (4.12)	Current density with time for cycles no 1, 10, 20, and 30 for Ni _{0.75} Ti _{0.25-y} Sn _y (NiO:Ti:Sn) with y values a) 0.01 b) 0.02 c) 0.03 d) 0.04 e) 0.05 f) 0.15 and g) 0.25.	72
Fig. (4.13)	Transparency for different layer NiO:Ti:Sn films.	76
Fig. (4.14)	Visible range Transparency (T) spectra for Glass, FTO/glass substrate, and different thickness films/substrate; air is set as a reference.	77

No.	Figure	Page
Fig. (4.15)	Coloration and bleaching transparency (T) spectra, during CV measurements (cycles 29 and 30), for double layer NiO:Ti:Sn with different Sn molar concentrations.	77
Fig. (4.16)	Transparency and current evolution during CV measurement for NiO:Ti:Sn _{0.03} layer. (→) indicates the current evolution and (- - - >) indicates corresponding Transparency evolution.	79
Fig. (4.17)	Transmission spectra with T _{max} and T _{min} for (a) FTO/glass substrate, (b) 1 layer film/substrate, and (c) 2 layer film/substrate.	81
Fig. (4.18)	Plot of $(\alpha E)^2$ versus photon energy E for different thickness NiO:Ti:Sn films deposited on glass substrate.	84

Electrochromic Properties of Sol-gel NiO –based films**By****Atheer Yousef Saleh Abu Yaqoub****Supervisors****Dr. Iyad Saadeddin****Co-Supervisor****Prof. Hikmat Hilal****Abstract**

Electrochromic films of NiO, Ni_{1-x}Ti_xO (with Ti nominal concentration ranging from 0-30 %) and Ni_{1-x}Ti_{x-y}Sn_yO (with Sn nominal concentration ranging from 1-5 %). Films of one and double imertion have been prepared by the sol-gel route using dip coating technique onto fluorine-doped tin oxide-coated glass substrates (FTO/glass). Characteristics of different films were studied in a comparative manner. Photoluminescence spectra, electrochromic behavior, cyclic voltammetry, transmittance spectrum, XRD and SEM have been investigated.

Our results indicate that electrochromic and other characteristics of the NiO can be enhanced by addition of Ti and Sn within NiO at certain concentrations. Mechanisms of coloration and morphology transformation of the layer during cycling in 0.5 M KOH electrolyte were discussed in terms of an activation and degradation period. Calculation of cathodic charge (Q_c), anodic charge (Q_a), optical density and coloration efficiency, energy gap, thikness were made and discussed.

Chapter One

Introduction

Chapter One

Introduction

1.1 Objectives

The main objective of this thesis is to enhance the electrochromic (EC) and crystal properties of NiO based electrochromic systems. This will be established by doping NiO with Ti and/or Sn species. Thin films of NiO doped with Ti and/or Sn nanoparticles, on fluorine-doped tin oxide (FTO) layer coated onto glass substrate, will be prepared using sol-gel technique. Different doping concentrations of Ti will be employed; 5-30 % in steps of 5% each. The optimum concentration of Ti species into NiO will then be decided. This depends on different results obtained from different performed experiments, and different experimental analysis. The crystal and electrochromic properties to be studied with different Ti concentrations include: (1) X-ray diffraction (XRD) analysis, (2) photoluminescence spectroscopy (PL), (3) scanning electron microscope (SEM), (4) thickness measurements, (5) Cyclic voltammetry (CV) and (6) Optical measurements.

The optimal concentration, of Ti onto NiO electrochromic material, will be used to apply co-doping of Ti and Sn within NiO. The effect of co-doping, onto electrochromic properties of the prepared electrochromic films, will be studied.

1.2 Why NiO based thin films?

Nickel oxide is one of the most popular electrochromic materials after tungsten oxide. As an anodic electrochromic material, nickel oxide has particular advantages owing to its high electrochromic efficiency. It can be used as a complementary electrode with WO_3 . Nickel oxide films have attracted special attention due to their good dynamic range (low potential operation range), cyclic reversibility (highly stable), durability and coloration, useful for smart windows technology [1-3]. Moreover, preparation of nickel oxide films by sol-gel method makes it possible to fabricate large area electrodes cheaply for industrial scale production.

1.3 Hypothesis

Electrochromic materials are commonly used as polycrystalline thin films. If doped with other substances, their crystal structures will be affected. Therefore, NiO films will be modified in their structure by doping them with SnO and/or TiO_2 substances. Such effects will be observed in the electrochromic properties of NiO based thin films. Moreover, effects on crystal and surface structure will be also observed.

1.4 Previous Studies

The interest in nickel oxide thin films is fast growing due to their importance in many applications in science and technology. Besides acting as an EC material, it can also be used as a functional layer material for gas sensors[4]. Stoichiometric NiO is an insulator with a resistivity of the order

of 10^{13} $\Omega\cdot\text{cm}$ at room temperature [5]. Its resistivity can be lowered by increasing Ni^{3+} ion concentration resulting from addition of monovalent ions such as lithium, by the appearance of nickel vacancies or by the presence of interstitial oxygen in the NiO crystallites [6].

Numerous studies have been performed in order to deduce the electrochemical mechanism which takes place during the coloration/bleaching process [7-9]. Recent study [10] reported that, in the activation period, an increase in capacity occurs, corresponding to chemical transformation $\text{NiO} + \text{H}_2\text{O} \rightarrow \text{Ni}(\text{OH})_2$. Structural changes from NaCl type (bunsenite NiO) to layered $\text{Ni}(\text{OH})_2$ occur upon amorphisation on the grain boundaries. In the steady state the reversible colour change from transparent to brownish involves the classical reaction $\text{Ni}(\text{OH})_2 + \text{OH}^- \rightarrow \text{NiOOH} + \text{H}_2\text{O} + \text{e}^-$. NiO grains act as a reservoir of the electrochemically active hydroxide layer [10]. Several papers reported that reversible electrochemical oxidation of Ni-atoms located at the NiO/electrolyte interface is responsible for a strong electrochromic effect [11-13], or that the electrochromic performance of nickel oxide depends on the size of the nanocrystallites [14-15]. Other earlier study [16] showed that the optical properties of a thin film, consisting of grains about 7 nm in diameter, are stable for at least 5000 cycles, whereas for a 17 nm grain size a significant degradation was observed only after 50 cycles. The decrease in electrochromic properties after prolonged cycling is associated with dissolution of the NiOOH phase structure [17]. Recent investigations regarding a nickel oxide counter electrode include deposition of a thin

protective layer on NiO when it is assembled together with WO_3 [18]. WO_3 is stable in acidic environments, but dissolves in basic media. On the other hand, Ni oxide is stable in a basic environment, but unstable in acidic ones. A possible solution is to add a protective layer on top of the NiO film [19].

Pure NiO layers showed a poor adhesion to the substrate, a permanent brown coloration after already 50 CV cycles and were easily degraded in the electrolyte [20,21]. However, Doping NiO with various dopants of various oxidation states was found to dramatically enhance the structure, the electrochromic properties, durability and adhesion of electrochromic NiO based layers [22-24]. Recently [25], Co-doping NiO with Ti and Zn was found to dramatically increase the electrochromic durability for the films upon cycling. Co-doping with Zn leads to creation of oxygen vacancies in the NiO film leading to better adhesion to the FTO substrate.

Electrochromic nickel oxide based thin films have been prepared by various physical methods (sputtering [11], pulsed layer deposition [17], electron-beam evaporation [26]) and chemical methods (atomic layer epitaxy [27], spray pyrolysis [28], anodic deposition [29] and sol-gel [30]). The films obtained differ in stoichiometry, structure, degree of crystallinity, crystallite size, etc. As a consequence, their electrochromic properties and colour efficiencies vary over a wide range. During or after the deposition process, the films have to be thermally treated in order to improve adhesion

to substrate and to ensure their structural stability during cycling in an alkaline electrolyte.

Electrochromic sol-gel NiO-TiO₂ layers have been recently developed and is formed to exhibit a fast switching time (<10 s), a deep reversible brown coloration, a much better stability and a better adhesion to glass substrates than pure NiO layers [31,32] (when cycled in KOH electrolyte). Also sol-gel NiO co-doped with Ti and Zn shows easier film preparation under ambient conditions [25]. This due to the remarkable delay in the hydrolysis process usually takes place when doping NiO with Ti.

Chapter Two
**Fundamentals and theoretical
background**

Chapter Two

Fundamentals and theoretical background

2.1. Chromism

Chromism is a process that induces a reversible change in the optical properties of compounds [33]. This phenomenon is induced by various external stimuli which can alter the electron density of substances. So, chromism can be classified according to the kinds of used stimuli. The major kinds of chromism are,

- **Thermochromism** is chromism that is induced by heat, i.e. temperature change.
- **Photochromism** is induced by light irradiation. This phenomenon is based on formation of light-induced color centers in crystals, precipitation of metal particles in a glass, or other reversible mechanisms. [33].
- **Electrochromism** is induced by gain and loss of electrons. This phenomenon occurs in compounds with redox active sites.
- **Solvatochromism** depends on the polarity of the solvent.

In Our study, we will uniquely consider electrochromism which constitutes the topic of the present work.

2.2. Electrochromism

2.2.1. Operation and applications of electrochromic devices (ECDs):

Design and Operation

Electrochromic materials (ECMs) modulate their optical properties depending on charge (electrons and ions) insertion/extraction [34-35] within the electrochromic material. The standard ECDs behave as thin film batteries which change their optical properties depending on insertion rate of charges in the ECM films. The electrochromic full device is composed of five superimposed layers on one substrate or positioned between two substrates in a laminate configuration (Fig. 1).

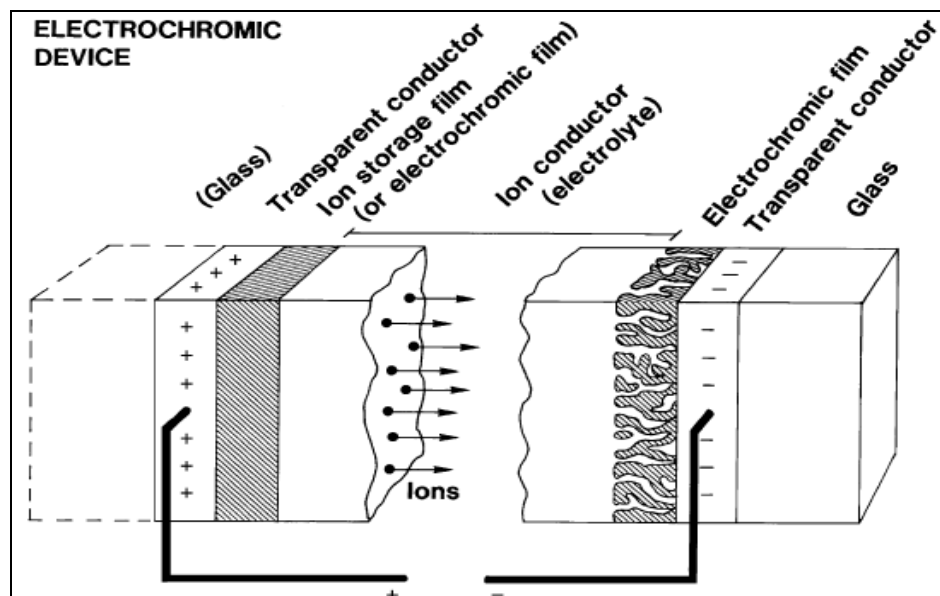


Fig. (2. 1): Basic design of an electrochromic device, indicating transport of positive ions under the action of an electric field

Normally, the substrates are made of glass or flexible transparent foil. The central part of the five-layer construction is a pure ion conductor (i.e., electrolyte) that can be organic (an adhesive polymer) or inorganic

(often based on an oxide film). The ions should be small in order to be mobile; protons (H^+) or lithium ions (Li^+) are normally preferred. This ion conductor is in contact with an electrochromic film (tungsten oxide being a typical example) capable of conducting electrons as well as ions. On the other side of the ion conductor is an electrochromic film serving as ion storage, ideally with electrochromic properties complementary to those of the first electrochromic film (Ni oxide being a typical example). The central three-layer structure is positioned between electrically conducting transparent films. In terms of optical and electrical properties, the most efficient transparent conducting layers are based on Sn-doped In_2O_3 (referred to ITO) and F-doped SnO_2 (referred to FTO) [35- 36]. FTO has the advantage of being less costly than ITO and readily available on large area glass panes.

When a voltage of the order of a few volts is applied between the transparent electrical conductors, ions are shuttled between the ion storage film and the EC film and simultaneously the electrons are injected (extracted) from the transparent conductors. The optical properties of the electrochromic thin films, and therefore of the electrochromic devices (ECDs) are thus modified. A reversal of the voltage, or short-circuiting, brings back the original properties. The ECD coloration can be controlled at any intermediate level, and the device exhibits open-circuit memory (like a battery).

Applications

ECDs are used in many practical applications (Fig. 2) such as electrochromic smart windows (ECW), smart sunroofs, rear-view mirrors, filters, smart glass wears, displays, etc.



Fig. (2.2): Various applications for ECD [37].

In term of energy saving, ECW, mostly used in buildings, is considered to be one of the most important applications. An ECW is illustrated in Fig. 3. It operates as shown in Fig. 1. When the electrochromic window is in its off-state (bleached or clear state), the visible light and part of solar heat energy (FTO or ITO films reflect part of infrared radiations) penetrate the ECW into indoors. The transmitted visible light and solar heat energy (from exterior to interior of buildings) can be minimized when the electrochromic window is in its on-state (colored or dark state)

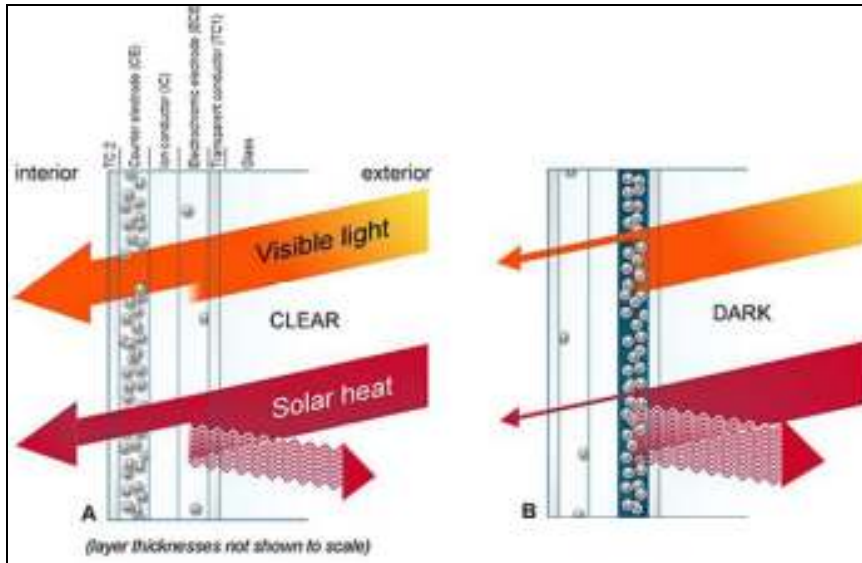


Fig.2. 3: ECWs with illustration of visible light and solar heat energy during operation.

2.2.2. Materials used in ECDs

Electrochromic devices cover a wide range of materials from conductive substrates to electrolytes and to electrochromic materials [38].

Transparent Conductive substrates

Due to the fact that the ECDs must be transmissive in the visible and conducts current, the substrate (glass or plastic) used in ECDs must be colorless, transparent as possible (>80%) in the visible domain, and electrically conductors. For this purpose, Several kinds of systems have been studied including metal grids or conductive polymers. However, the most used by far are the Transparent Conductive Oxides (TCO) deposited on glass or plastic [38-40]. n-type TCO thin films are generally based on $\text{In}_2\text{O}_3:\text{Sn}$ (ITO) and $\text{SnO}_2:\text{F}$ (FTO) using commonly deposition techniques of PVD and CVD, respectively. Recent investigations report resistivities as low as $6 \times 10^{-5} \Omega \cdot \text{cm}$ for ITO films [41]. Films of $\text{ZnO}:\text{Al}$ (or ZnO based)

are currently attracting much attention as a consequence of the rising prices of In.

Electrolytes

The electrolyte, as pure ion conductor and electronic insulator, can be organic or inorganic, liquids or solids. The ions should be small in order to be mobile, proton (H^+) or lithium ions (Li^+) are generally preferred. Proton conductors are commonly associated with higher ionic conductivity whereas lithium-based electrolytes show higher stability in a larger electrochemical active window and limited film dissolution partially linked to the absence of water or H_2 or/and O_2 formation. The ionic conductor (electrolyte) must be also transparent, neutral coloring, and should not react with the two insertion electrochromic electrodes in between it is sandwiched. This chemical stability must be ensured both during deposition and cycling. Solid-ion conducting electrolytes for use in ECDs are listed in Table 1. Inorganic electrolytes are often based on oxide thin films which serve as media for cation conduction. Organic electrolytes fall in two categories, polymer electrolytes and polyelectrolytes; Polymer electrolytes are macromolecules containing dissolved Li salt or acid [34] depending on the needed ion transport. Polyelectrolytes are polymers containing ion-labile groups.

Table (2. 1): Some Solid ion-conducting electrolytes for use in ECDs [42]

Electrolytes	
Inorganic electrolytes	Organic polymers
LiAlF ₄	Nafion™
LiNbO ₃	Poly(acrylic acid)
Sb ₂ O ₅ (inc. HSbO ₃)	Poly(AMPS)
HSbO ₃ based polymer	Poly(methyl methacrylate)
Ta ₂ O ₅ (including « TaO _x »)	PMMA (« Perspex »)
TiO ₂ (including « TiO _x »)	Poly(2-hydroxyethyl methacrylate)
H ₃ UO ₃ (PO ₄).3H ₂ O (« HUP »)	Poly(ethylene oxide), PEO
ZrO ₂	Poly(vinyl chloride), PVC

Electrochromic materials (ECMs)

There are many types of ECMs, such as organic, inorganic, and metal organic complexes.

- Organic materials

A large number of electrochromic organic dyes and derivatives are known. They include bipyridinium systems, carbazoles, methoxybiphenyl, quinines, diphenylamine, pyrazolines [43]. Extensive literature reports are made on bipyridinium compounds and particularly on 1,1'-dimethyl -4,4'-bipyridinium, also called methyl viologen [44]. They can be either used as such by solubilising in the electrolytic solution or as solid films after polymerisation or grafting onto an appropriate substrate. Organic materials also include conductive polymers. As opposed to inorganic ECMs, organic ECMs usually take advantage of very high coloration efficiencies (hundreds of cm²/C), fast switching time and wide color ranges. They can be either anodically or cathodically colored.

- Inorganic materials

Inorganic EC materials are especially important in electrochromic technology because of their highly stable properties, potential and wide applications [45-46]. So far, much effort has been focused on transition metal oxides based on tungsten (W) [47], molybdenum (Mo) [48], vanadium (V) [49], titanium (Ti), iridium (Ir), and nickel (Ni) [50-51]. Most of the metal oxides known so far have structures built from MeO_6 octahedra with a Me transition metal at the center. A list of inorganic electrochromic materials is reported in Table 2.

Table (2.2): Properties of the most studied electrochromic inorganic materials.

oxide	Coloration: Cathodic (C) or Anodic (A)	Oxidized	Reduced	Ref.
WO_3	C	Colorless	Blue	52
TiO_2	C	Colorless	Blue	53
Li_xCoO_2	A	Deep blue	Blue	54
MoO_3	C	Colorless	Blue	55
V_2O_5	C	Pale yellow	Pale Blue	56
IrO_x	A	Blue/Gray	Colorless	57
Nb_2O_5	C	Colorless	Brown	58
NiO	A	Brown/black	Colorless	59
$\text{InO}_2:\text{Sn}$	C	Colorless	Brown (irreversible)	60

All of electrochromic materials exist in different phases and have crystalline, polycrystalline or amorphous structures associated with different colored/bleached mechanisms. Among the ECMs in Table 2.2, WO_3 and 'NiO' are typical examples of cathodic and anodic ECMs respectively. In fact, nowadays precisely, interest is becoming more

focused on electrochromic devices based on WO₃ and 'NiO' thin films due to their complementary coloration (blue for reduced 'WO₃' and brown for oxidized 'NiO') [59]. Intensive work has been first reported on rigid (glass-based) devices [52], then on flexible (polyester film-based) devices.

In addition to inorganic oxides, a new family of inorganic non-oxide electrochromic materials was demonstrated [53]; hexacyanometallates compounds of the general type $M_k[M'(CN)_6]_l$, where M and M' are transition metal ions with different vacancies can exhibit pronounced anodic coloration. One of the best examples is the case of Prussian Blue, PB [54].

If NiO thin films experience strong electrochromic effect in KOH electrolyte, they show, unfortunately, low cycling durability in such electrolyte [55-57].

2.2.3.Types of electrochromic devices (ECDs)

ECDs can be classified in three types, solution, hybrid and battery-like types, as shown in Fig. 4. For solution and hybrid type ECDs, at least one electrode should be solution or gel-type electrolyte. The ECDs are self-erased under open circuit potential (meaning no memory effect). On the other hand, battery-like devices have a good memory effect under open circuit potential (like a battery in fact). Coloration of the two electrodes, in battery-like devices, complements one another, thus showing their electrochromic superiority to the solution and hybrid types [38].

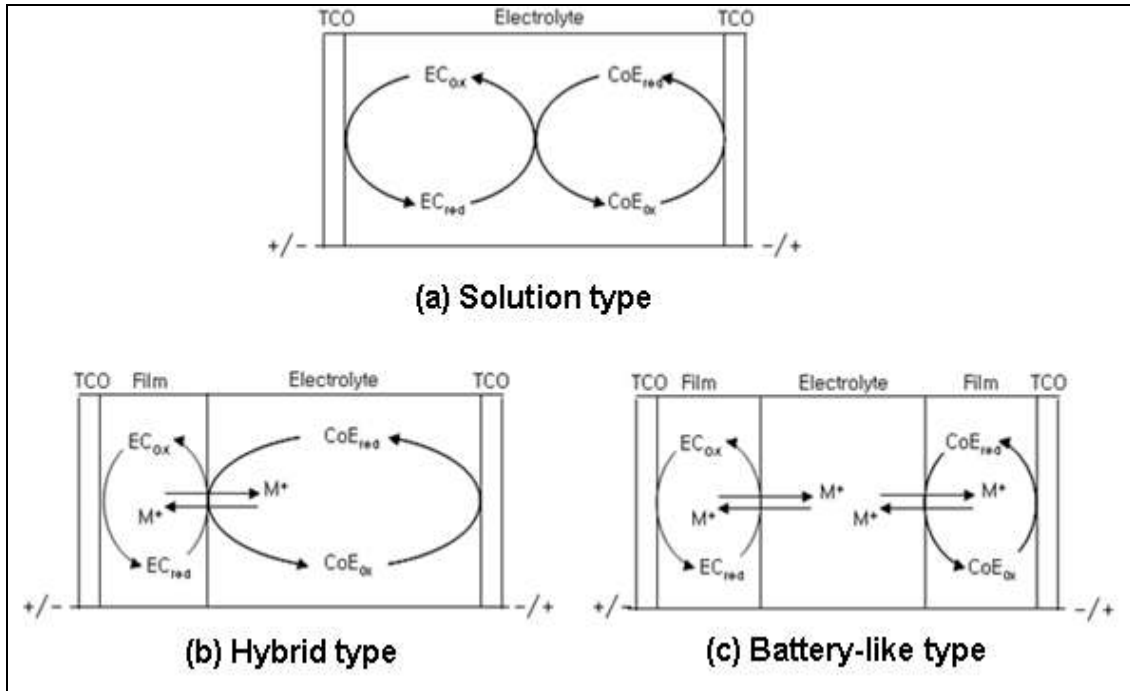


Fig (2. 4): Three different types of electrochromic devices (ECDs): (a) solution type, (b) hybrid type, and (c) battery-like type.

2.2.4. Electrochromic device (ECD) features

Color change in the visible light is one important feature of electrochromic devices. Equation (1.1) expresses the contrast ratio (CR):

$$CR = R_o / R_x \quad (2.1)$$

R_x and R_o represent reflected light intensity in bleached and colored states, respectively. Higher value of CR indicates larger difference in transmittance. Therefore, we could evaluate a given electrochromic device with its CR, together with its absorbance, Absorbance, A , is equal to change of optical density $\Delta OD (\lambda)$,

$$A = \Delta OD (\lambda) = \log T_b/T_c \quad (2.2)$$

where T_b and T_c represent transmitted light intensity in bleached and colored states, respectively. The change in optical density, $\Delta OD(\lambda)$, can also be expressed by [58],

$$\Delta OD(\lambda) = \eta Q = CE \cdot Q \quad (2.3)$$

Q is the injected electronic charge per unit area needed to switch the electrochromic thin film material from bleached to colored state. η indicates the coloration efficiency, which is also expressed in the literature as CE (cm^2/C). Therefore, CE is proportional to ΔOD and inversely proportional to the quantity of electric charge per unit area.

An electrochromic device with high coloration efficiency provides big difference in transmittance with small amount of electric charge. The most representative inorganic thin film electrochromic materials such as WO_3 and NiO have coloration efficiency (CE) of $\sim 40 \text{ cm}^2/\text{C}$, whereas organic electrochromic thin films, such as PEDOT, show more than $100 \text{ cm}^2/\text{C}$ in CE [38].

Electrochromic devices are also evaluated based on response time. Generally we measure the time needed to reach 90 % of bleached/colored state. Electrochromic devices show lower response times than those for liquid crystal displays (LCDs). However, the lower response time is not limiting for building since long cycling life is also required for ECDs.

2.2.5. Benefits with electrochromic windows (ECWs)

Due to its optical modulation properties, the ECWs deliver the following benefits [59-60];

- Block solar heat; capable to provide up to 40% on energy bills [59].
- Always keep a view and connection to the outdoors; ECW is transparent in its color state.
- Block glare; always provide a climate that makes the human relax
- Dramatically reduce fading; ECWs block not only nearly 100% of the UV radiation, but also the portion of visible light that causes fading.

2.3. Background on nickel compound

2.3.1. Nickel and nickel compounds [61]

Nickel is a hard, malleable, silvery white, ferromagnetic metallic element. Nickel is a Group VIII B element, with atomic number 28 and atomic mass 58.69 g/mol. The melting point for nickel is $\sim 1,453$ °C and the boiling point is $\sim 2,732$ °C. Nickel has different oxidation states (0, 1+, 2+, 3+, and 4+). The electronic configuration for nickel is $[\text{Ar}]4s^23d^8$. Magnetic and chemical properties of nickel resemble those of iron and cobalt. So, it easily forms a number of alloys such as nickel-iron, nickel-copper, nickel-chromium, nickel-zinc and others. Nickel compounds mostly have blue or green colors. Nickel could be combined with many other elements, including chlorine, sulfur and oxygen. Many nickel compounds dissolve

readily in water forming characteristic green or blue colors. Nickel compounds are used in electrochromic device, coloring ceramics, batteries and chemical reaction catalysts.

2.3.2. Nickel(II) oxide, NiO

The mineralogical form of NiO bunsenite is rare. Therefore, it must be synthesized. There are many kinds of routes to synthesize NiO. Among those, the most well known route is pyrolysis of Ni²⁺ compounds such as hydroxide, nitrate, and carbonate, which yield a light green powder. Heating under oxygen or air atmosphere leads to black 'NiO' powder, which indicates a non-stoichiometry [62]. NiO belongs to NaCl structure, so-called rock salt structure. The space group of NaCl structured NiO is Fm3m with lattice parameters $a = 4.1769 \text{ \AA}$ (JCPDS, 47-1049). 'NiO' is often non-stoichiometric. The non-stoichiometry is accompanied by a color change from green to black due to the existence of Ni³⁺ resulting from Ni vacancies [65]. This leads to p-type conductivity. In order to explain optical absorption gap in NiO, there are two main theories, which deal respectively with $p \rightarrow d$ transitions from oxygen to nickel (charge transfer) and cationic $d \rightarrow d$ transitions [66]. NiO and NiO-derived materials have been used in many applications such as fuel cells, secondary ion batteries, dielectric materials and others, which accounts for the ~ 4000 ton annual production of NiO [67]. With regard to toxicity, long term inhalation of NiO causes health risks such as lung cancers [68].

2.3.3. Nickel hydroxide, Ni(OH)₂

There are mainly two phases of nickel (II) hydroxide [Ni(OH)₂] which are α and β types. The two different phases are illustrated in Fig. 5. β -Ni(OH)₂ crystallizes in the hexagonal system which is described as a hexagonal close-packed (hcp) structure of hydroxyl ions (AB oxygen packing) with Ni(II) occupying half the octahedral interstices. This structure is in fact a layered structure. Each layer consists of hexagonal planar arrangement of Ni(II) ions with an octahedral coordinated oxygen. The layers are stacked along the c-axis with interlayer distance being 4.6 Å.

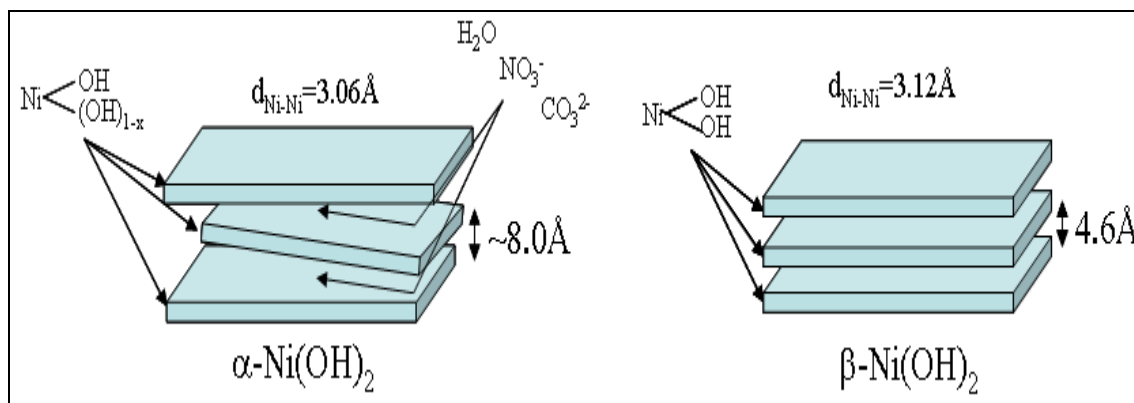


Fig. (2. 5): Illustration of α -Ni(OH)₂ and β -Ni(OH)₂ phases [69].

The α -Ni(OH)₂ structure is a hydrated form of the β -Ni(OH)₂ phase. As illustrated in the left panel of Fig. 5, some guests such as water, NO_3^- , and CO_3^{2-} are intercalated in the Ni(OH)₂ slabs resulting in higher distance between them ($\sim 8.0 \text{ \AA}$). A great variety of α -type hydroxides can be obtained depending on the degree of hydrated turbostratic hydroxide. The variety occurs between a highly turbostratic α -Ni(OH)₂ and the well stacked β -Ni(OH)₂, as proposed by Le Bihan *et al.* [70]. Fortunately, both

types of $\text{Ni}(\text{OH})_2$ are transparent in their thin film form with a band gap of about 3.7 eV[71].

2.3.4. Nickel oxyhydroxide, NiOOH

There are two basic types of layered nickel oxyhydroxide, NiOOH, which are β [72] and γ -NiOOH [73]. As shown in Fig. 6, β -NiOOH is considered as a relatively well defined material compared to γ -NiOOH. Water and alkali ions (mostly K^+ and Na^+) are intercalated in the ‘ NiO_2 ’ layers. The range of oxidation state of nickel in ‘ γ -NiOOH’ is between 3 and 3.75. Nevertheless, β - and ‘ γ -NiOOH’ have distinct inter-sheet distances which are 4.7 and 7.0 Å, respectively (Fig. 6). Both types of NiOOH are brownish in thin film form which is very practical in the application of electrochromic devices as an active counter electrode.

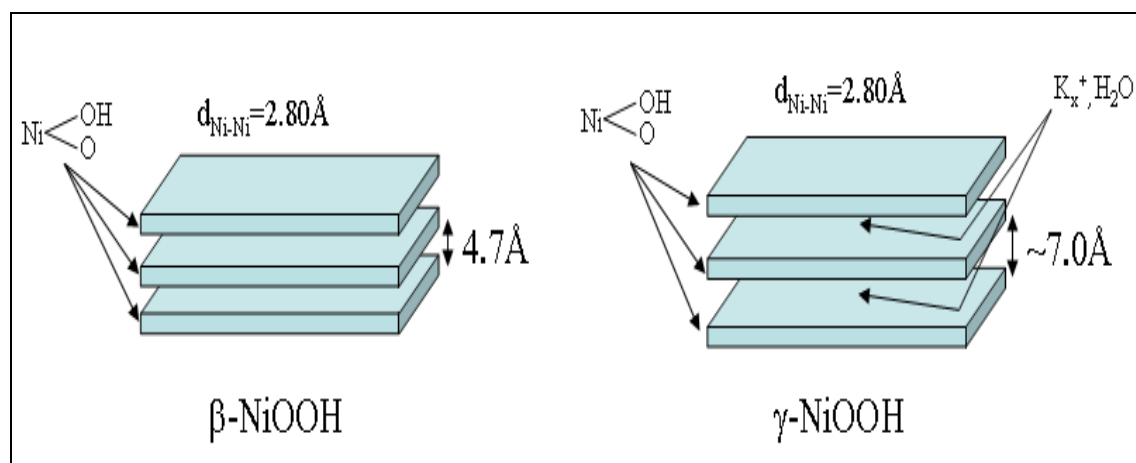


Fig (2. 6): Illustration of β -NiOOH and γ -NiOOH phases [69].

2.3.5. Coloration mechanism of nickel oxide-based thin films.

Chemical and electrochemical properties of nickel oxide-based thin films have been mainly investigated in alkaline electrolyte, mostly aqueous

KOH electrolyte. The surface of NiO particles is converted into Ni(OH)₂ when immersed in KOH electrolyte as shown in the schematic below (Figure 7). The electrochemical reaction of the Ni(OH)₂ and NiOOH then take place (when potential is applied) representing the electrochromic behavior between bleached and colored states.

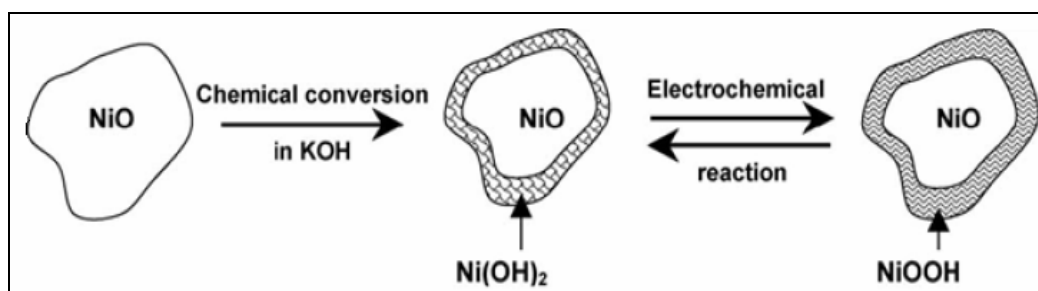


Fig. (2. 7): Schematic diagram for NiO under chemical and electrochemical reaction.

The general oxidation/reduction reaction for hydrated NiO electrode in aqueous KOH electrolyte as proposed by Bode *et al.* [74] is shown in Figure 8. The Bode scheme represents the transition between Ni(II) and Ni(III) as a main feature. Fig. 8 shows the two main oxidation/reduction reactions which are the α -Ni(OH)₂/ γ -NiOOH (α/γ) and β -Ni(OH)₂/ β -NiOOH ($\beta^{\text{II}}/\beta^{\text{III}}$) transformations [69]. β -Ni(OH)₂ and β -NiOOH phases are observed during cycling [75-77]. However, one can also observe the formations of the γ phase [72] and other intermediate phases [73-77]. The transformation from β -NiOOH to γ -NiOOH, which is irreversible, results from an overcharge of β -NiOOH.

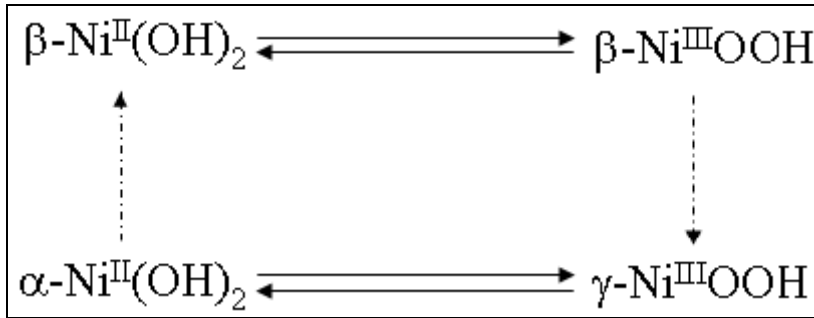
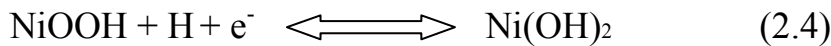


Fig. (2. 8): The general reaction scheme proposed by Bode *et al.* [74].

The other reduction/oxidation chemical reaction deals with α/γ transformation where at least 1.3 electrons may be transferred [72,78].

Among all mechanisms proposed so far for nickel oxide thin films in aqueous basic electrolytes [69,17,3,80], equations (2.4) and (2.5) illustrate the generally accepted electrochromic mechanisms [44].



bleached state

colored stat

2.4. Optical properties

-Film thickness

Transmission spectra of the films provide a powerful tool to determine the thickness of transparent thin films.

Consider a thin film of refractive index n deposited on a transparent substrate of refractive index n_1 (figure 2.9). From the transmission

spectrum, measured at normal incident, for the transparent substrate, the reflective index of the substrate can be calculated using [81]

$$n_1 = \frac{1}{T_s} + \left(\frac{1}{T_s^2} - 1 \right)^{1/2} \quad (2.6)$$

where T_s is the interference-free transmission of the substrate.

In the case transparent thin films on a transparent substrate, two regions can be distinguished in the UV-visible range: a strong absorption region and interference transmission region (Fig. 2.10).

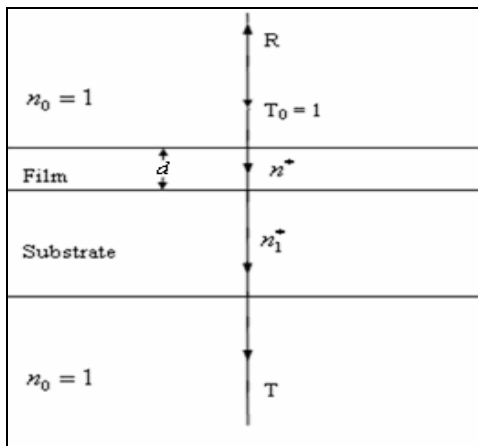


Fig. (2.9): System made of an absorbing thin film on a thick finite transparent substrate.

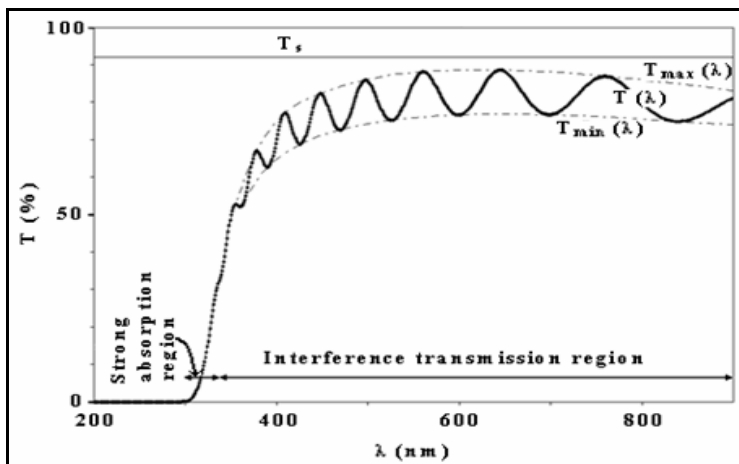


Fig. (2.10): Typical transmission spectrum for a uniform TCO thin film.

The maxima and minima of $T(\lambda)$ shown in figure. 2.10 occur for [82-83]

$$2nd = m\lambda \quad (2.7)$$

where m (the order number) is an integer for maxima and half integer for minima and d is the film thickness. The real part of the complex refractive index is expressed by the following equation:

$$n = [F + (F^2 - n_0^2 n_1^2)^{1/2}]^{1/2} \quad (2.8)$$

where

$$F = \frac{n_0^2 + n_1^2}{2} + 2n_0 n_1 \frac{T_{\max} - T_{\min}}{T_{\max} T_{\min}}$$

with n_0 and n_1 which are respectively the real part of the refractive index of the air and substrate. Equation (2.8) shows that n is explicitly determined from T_{\max} , T_{\min} (shown on figure 2.10), with n_1 and n_0 being measured at the same wavelength. Knowing n , one can also find the film thickness, which can be calculated from the two successive maxima or minima using the relation (2.7), and is given by

$$d = \frac{\lambda_1 \lambda_2}{2[n(\lambda_1)\lambda_2 - n(\lambda_2)\lambda_1]} \quad (2.9)$$

where λ_1 and λ_2 are the wavelengths of two successive maxima or minima.

2.5. Deposition techniques of NiO–based thin films

Electrochromic NiO thin films can be prepared by many techniques. The major methods are categorized into physical, chemical and electrochemical ones.

2.5.1 Physical Techniques

(a) Sputtering

Sputtering is considered as the most common physical vapor deposition (PVD) techniques used for thin films depositions. Preparing electrochromic Nickel oxide thin films by started in 1986 [84]. A schematic diagram showing the rf reactive magnetron sputtering is shown in Fig. 11. Later DC reactive magnetron sputtering techniques have been also used [85-86]. The sputtering process involves the creation of gas plasma (usually an inert gas such as argon) by applying voltage between a cathode and an anode. The cathode is used as a target holder and the anode is used as a substrate holder. Source material is subjected to intense bombardment by argon ions. By momentum transfer, particles are ejected from the surface of the cathode and they diffuse away from it, depositing a thin film onto a substrate.

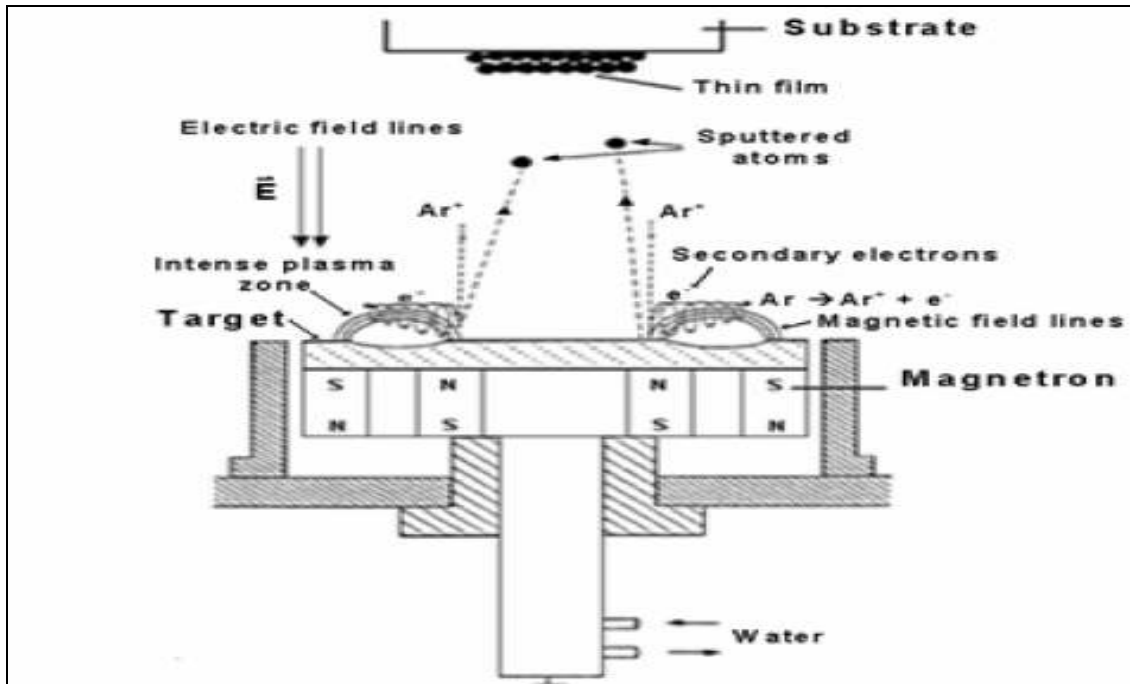


Fig (2. 11): Schematic presentation of Principles of the rf magnetron sputtering [40].

(b) Electron beam evaporation

Electron beam evaporation is a form of PVD in which NiO-based electrochromic thin films can be formed [87]. In this technique, an electron beam given off by a charged tungsten filament under high vacuum. By means of magnetic fields and/or electric fields, the formed electron beam is deflected and accelerated towards the anode material to be evaporated. When the electron beam strikes the target surface, the motion kinetic energy is transformed by impact into thermal energy (heat). This causes atoms from the target to transform into the gaseous phase. These atoms then precipitate onto substrate forming solid material thin film. Figure 12 shows a schematic diagram for the electron beam evaporation technique.

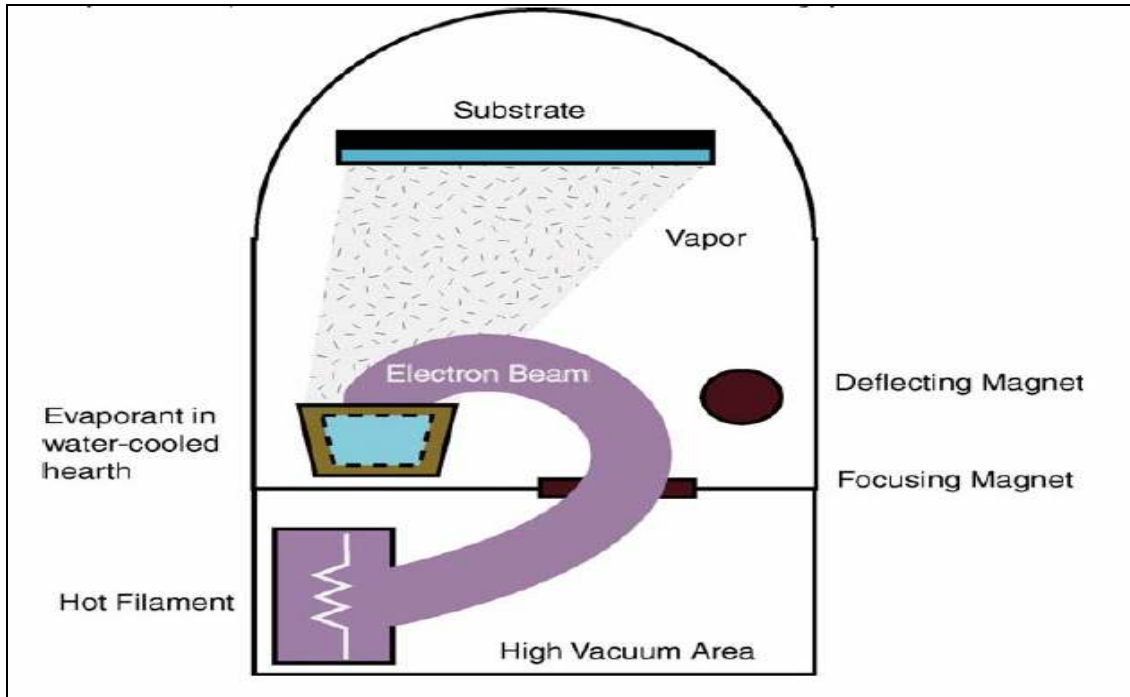


Fig (2.12): A schematic shows the electron beam evaporation technique

c) The Pulsed laser deposition technique (PLD)

PLD is a PVD technique for film deposition [88-89] in which a high power pulsed laser beam is focused inside a vacuum chamber to hit a target. Material is vaporized from the target inducing a plasma plume. This plasma plume reaches the substrate ($\text{SnO}_2\text{:F}$ (FTO) or $\text{In}_2\text{O}_3\text{:Sn}$ (ITO)) depositing the thin film. Film deposition process may occur under high vacuum or a background gas atmosphere. A typical configuration of a PLD deposition chamber is illustrated in Fig. 13.

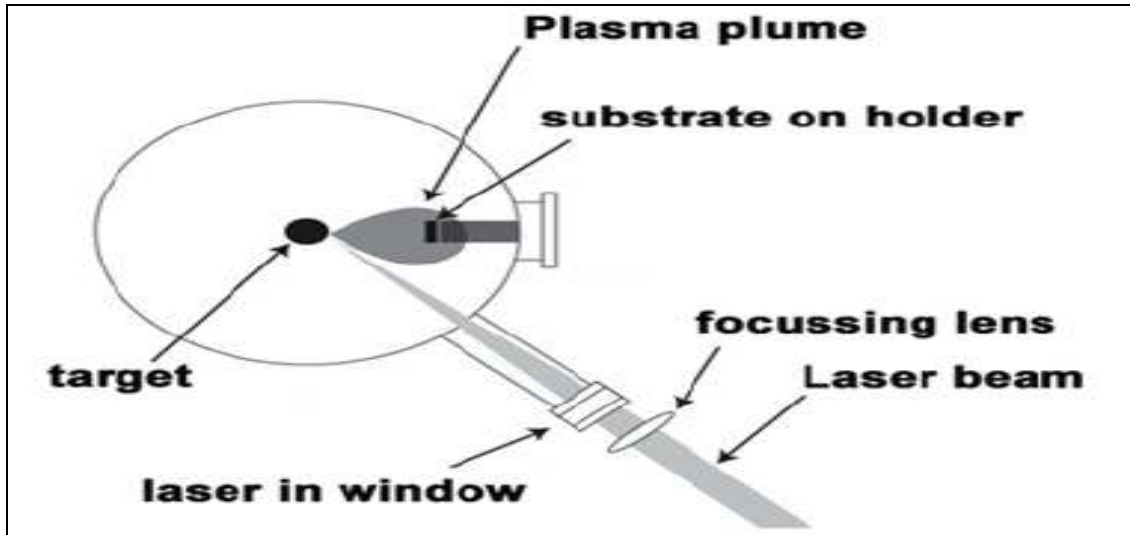


Fig (2. 13): A typical configuration of a PLD deposition chamber.

The main factors that influence deposition thickness and crystallinity are

- a) the target material (composition, density), b) the laser energy,
- c) the laser frequency d) the distance from target to substrate and
- e) the gas nature and pressure inside the chamber (Oxygen, Argon, etc.)

2.5.2 Chemical Techniques

Vacuum techniques, typically sputtering, evaporation and pulse laser deposition need high vacuum which makes them expensive methods. Wet chemical deposition is an alternative method for producing amorphous thin films with high surface area [34]. The problem facing this method is the lack of soluble nickel alkoxide.

(a) Electrochemical Deposition (ECD)

The major advantages of the electrodeposition technique are:

(i) large area manufacturing. (ii) very low manufacturing cost. (iii) compatibility with a variety of substrates. The experimental arrangement for film preparation is shown in Figure 14. It involved a solution containing chemical materials & distilled water, HCl to control the value of pH.

The solution temperature was maintained in a constant temperature oil bath and under constant stirring during deposition [90]. The pre-cleaned substrate, with dimensions $1 \times 4 \text{ cm}^2$, and the platinum plate were held by holders and partially immersed in the chemical solution. The system was firmly closed under a continuous flow of nitrogen. Deposition was performed by an applied potential of a DC stripping.

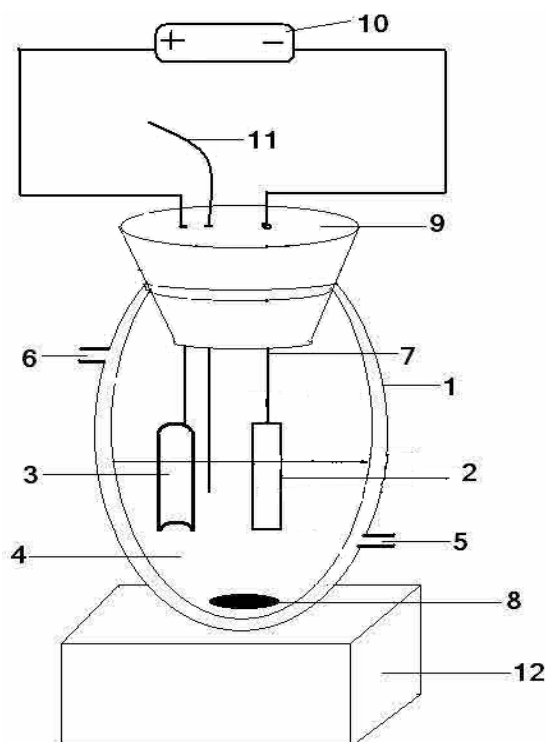


Fig. (2.14): Experimental arrangement for film growth in ECD.

1- Beaker (60 ml) ; 2- FTO/Glass substrate; 3- platinum electrode;
4- solution containing 5- paraffin oil input for the constant-temperature

bath; 6-paraffin oil output for the constant -temperature bath; 7-substrate holder; 8-magnetic stirrer; 9-rubber seal; 10- power supply; 11-nitrogen; 12-magnetic stirrer plate The substrate was connected to the cathode, and the platinum plate was connected to the anode of the power supply.

b) Chemical Bath Deposition (CBD)

Thin films were deposited on FTO/Glass substrates using CBD technique. The experimental setup for the film preparation is shown in Figure 15. It involves a chemical bath containing of stirred de-ionized water with many chemicals materials. The bath has a constant temperature water bath under constant stirring during deposition [91] .

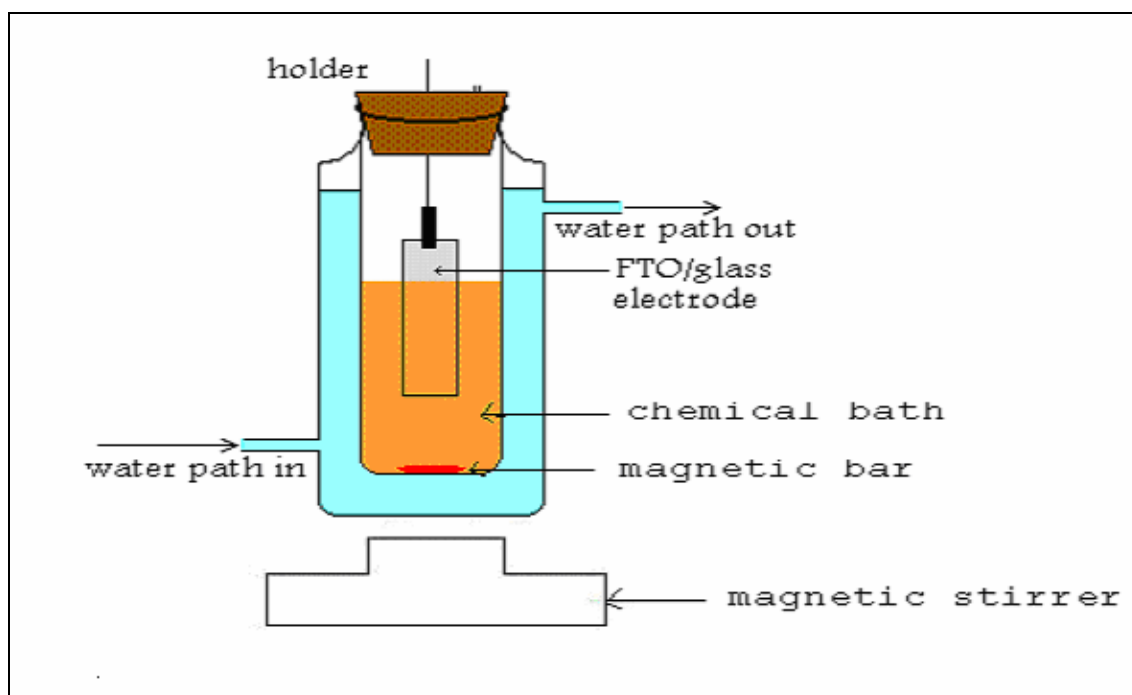


Fig. (2.15): Experimental setup for the chemical bath

The pre-cleaned FTO/Glass substrates, with dimensions $1 \times 4 \text{ cm}^2$, were held by a substrate holder and covered with Teflon. The substrates

were then partially immersed in the solution. The system was firmly closed using a rubber seal. After deposition, the coated substrate was cleaned with distilled water and dried with N₂ atmosphere.

(c) Spin Coating (SC)

The solution (sol-gel solution for instant) is placed on the substrate and then the substrate is rotated in order to spread the solution by centrifugal force. At this stage, gas blowing toward the substrate during rotation can be used. The film thickness can be controlled by varying rotation speed, rotation time and coating solution viscosity. The used solvent is usually volatile and simultaneously evaporates. The machine used for spin coating is called a spin coater or spinner. A coating process using spin coater or spinner is illustrated in Fig.2. 16.

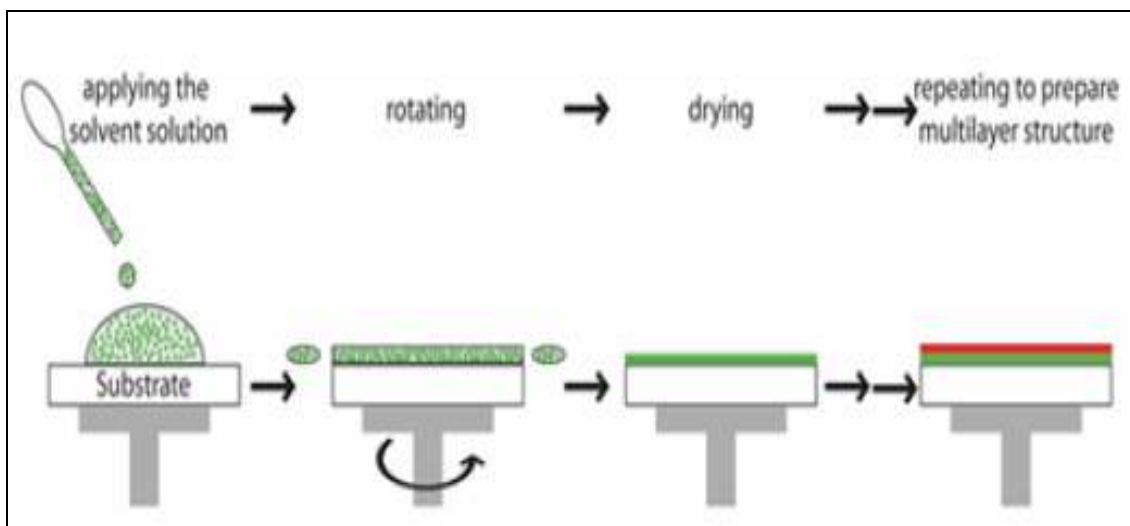


Fig. (2. 16): A spin coating process: applying the solution onto the substrate, rotating the substrate and drying. Repeating this process leads to multilayer structure.

(d) Dip Coating

Dip coating is a technique which is practical and economic for thin film deposition at industrial scale [92-94]. Figure 17 represents dipping of the substrate into the coating solution (sol-gel solution for instance), wet layer formation by withdrawing the substrate and gelation of the layer by solvent evaporation.

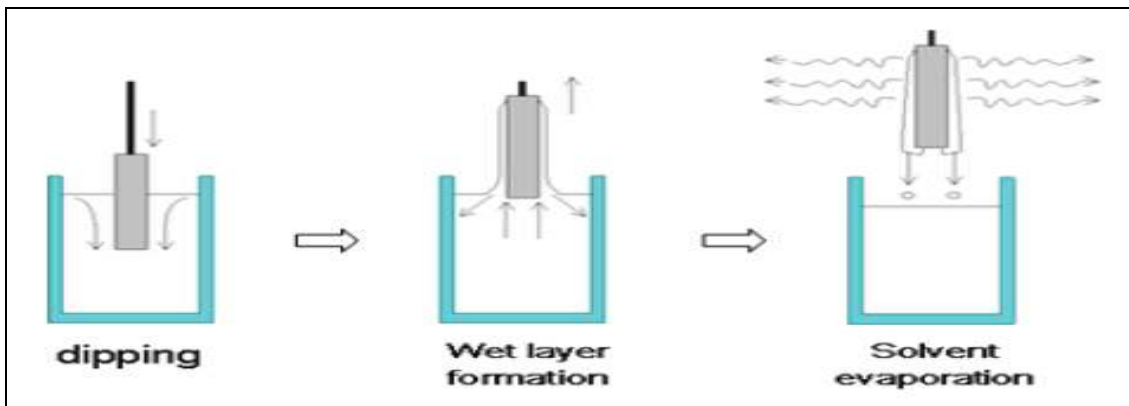


Fig (2. 17): Schematic shows the stages of the dip coating process

The substrate is first immersed in the coating solution at constant speed. The substrate is then aged inside the solution and then pulled up. The thin film grows on the substrate during pulling up at constant speed. Finally the pulled-up substrate is aged in the air to evaporate the solvent from the liquid, forming thin film. The film thickness (h), which depends on the withdrawal speed (v) and the viscosity of the coating solution (η), can be determined using the Landau-Levich equation (2.10) [94].

$$h = 0.94(\eta \cdot v)^{2/3} / \gamma_{LV}^{1/6} (\rho \cdot g)^{1/2} \quad (2.10)$$

where γ_{LV} = liquid-vapor surface tension, ρ = liquid density and g = gravity.

2.5.3 Sol-gel process

The meaning of “sol-gel” originated from “sol” indicating the evolution of inorganic networks through the formation of a colloidal suspension and “gel” corresponding to the gelation of the sol to form a network in a continuous liquid phase. Sol-gel method is widely employed to deposit thin films, to synthesize nanomaterials and ceramics. The typical steps involved in sol-gel processing are shown in the schematic diagram below (Fig. 18) [95].

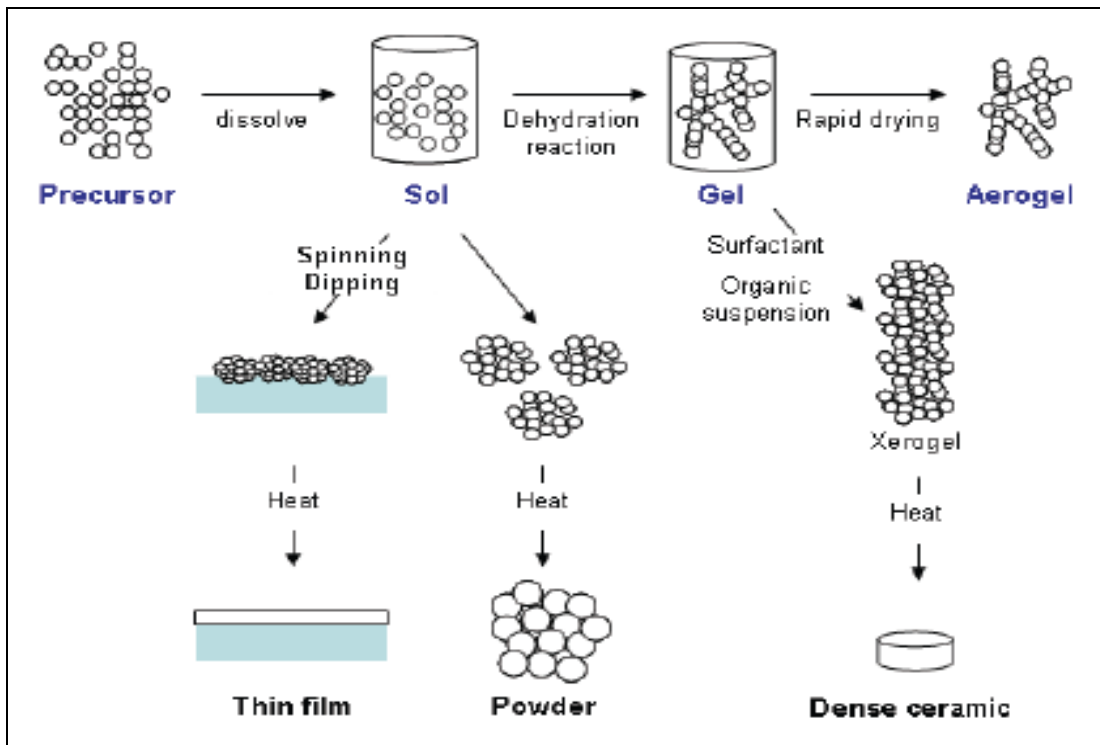


Fig. (2. 18): Schematic representation of sol-gel process to synthesize thin films, nanomaterials and ceramics.

Chapter Three
Experimental Work

Chapter Three

Experimental Work

3.1 Materials and film preparation

3.1.1 Chemicals and Solvents

In its pure form, materials are purchased from different companies:

- 1) Titanium(IV) Isopropoxide [$\text{Ti}\{\text{OCH}(\text{CH}_3)_2\}_4$], and Tin (II) Chloride dihydrate [$\text{SnCl}_2 \cdot 2\text{H}_2\text{O}$] were purchased from Alfa Acer.
- 2) Nickel (II) Acetate Tetrahydrate [$\text{Ni}(\text{CH}_3\text{COO})_2 \cdot 4(\text{H}_2\text{O})$] was purchased from Aldrich.
- 3) Potassium hydroxide (KOH) is from Frutarom.
- 4) Other materials like ethanol, methanol, and hydrochloric acid (HCl) are self packing locally.
- 5) Highly conductive and transparent in the visible Fluorine-doped tin dioxide on glass (FTO/ glass) samples were used as substrates. They were kindly donated by Dr. Guy CAMPET from ICMCB-CNRS, University of Bordeaux I, Bordeaux, France.

3.1.2 Substrate Cleaning Process

FTO/glass substrates with dimensions of $5 \times 1 \text{ cm}^2$ were prepared to deposit NiO-based electrochromic films. In order to obtain good adherence and uniformity for the films, it is necessary to use pre-cleaned substrates, The FTO/glass substrate cleaning steps were as follows:

- 1) Washing with liquinox soap to clean any dusts or attachments.
- 2) Washing with deionized water to remove soap
- 3) Washing with methanol to dissolve any oily attachments and left to dry
- 4) Shaking in dilute HCl(10%) for 5 seconds to dissolve any un-cleaned attaches
- 5) Washing with deionized water again
- 6) The substrates were then left to dry in air to be used in sol-gel /dip-coating process.

3.1.3 Preparation of NiO based films

Two types of NiO-based electrochromic films (NiO doped with Ti and NiO doped with both Ti and Sn) were grown using sol-gel solutions. The prepared sol-gel solutions were deposited on the pre-cleaned FTO/Glass substrate by using dip coating process [25, 31]. The steps of dip coating process for NiO-based films is shown in Figure 3.1 and summarized as follows:

- 1- Immersion FTO/glass substrate in the sol-gel with a speed of 2.5 mm/s. Note that part of the substrate was not immersed in solution for electrical contact with FTO.
- 2- The substrate left suspended in the solution for 10 min to ensure good exposure of the substrate to film.

- 3- Drawing out the FTO/Glass/film with speed of 2.5 mm/s
- 4- To allow homogeneous film growth, to drop any extra thick parts from the film surface and to evaporate unwanted solvents the FTO/Glass/film was left above the sol-gel beaker, for 10 min.
- 5- The slides were left for one day under air to dry .
- 6- Samples were annealed at 350°C for 1.5-2 hours under air pressure.
- 7- For thicker films we made multiple immersion (depending on desired thickness) by repeating steps 1-4 and then annealed at 150-200°C for 15 min to evaporate H₂O before coming finally to step number 5.

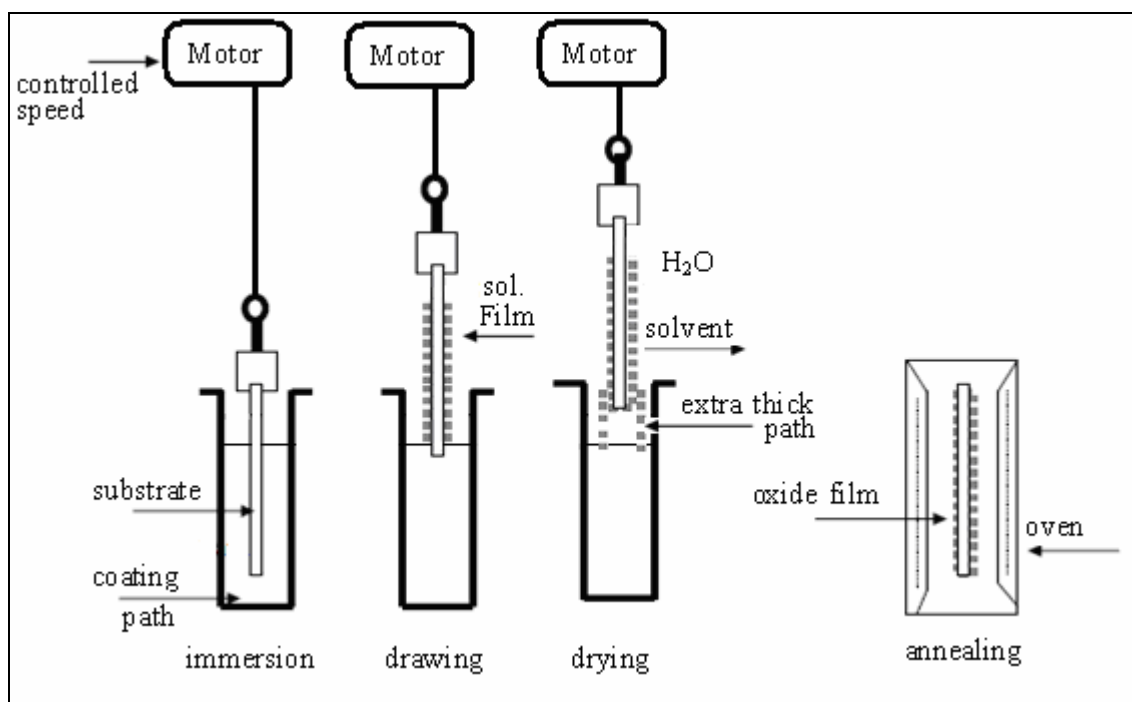


Fig (3.1): Steps of NiO-based films deposition by dip coating process.

Two different preparation procedures for sol-gel solutions were used depending on the film composition:

a) Sol-gel solution for NiO doped with Ti (NiO:Ti) films

The films were prepared using sol-gel route in order to prepare NiO:Ti. The titanium was assumed to compensate Ni in the NiO structure, after annealing, according to “Ni_{1-x} Ti_xO” [25,31].

0.5 M sol-gel solution of Ni_{1-x} Ti_xO was prepared in 40 ml ethanol; with Ti molar concentration varies from 0.0 - 0.3 in steps of 0.05 (see table 3.1). Firstly Ni(CH₃COO)₂.4(H₂O), with appropriate molar concentration, was added to 30 ml of ethanol and stirred by magnet for 6 hours as a result transparent green color was obtained. Meanwhile, Ti-isopropoxide was added to 10 ml of ethanol and stirred for 30 min. Both mixtures was then mixed and also stirred for 30 min. The intended composition, after annealing, and the masses of each material used in sol-gel preparation for different concentration are listed in table1 below:

Table (3.1): list of intended composition, nickel (II) acetate mass, and Ti-isopropoxide mass used in the sol-gel preparation. All sol-gel solutions were prepared in ethanol total volume of 40 ml.

Sample no.	composition	Nickel (II) acetate (gm)	Ti-isopropoxide (gm)
1	NiO	4.98	0
2	Ni _{0.95} Ti _{0.05} O	4.73	0.28
3	Ni _{0.90} Ti _{0.10} O	4.48	0.57
4	Ni _{0.85} Ti _{0.15} O	4.23	0.85
5	Ni _{0.80} Ti _{0.20} O	3.98	1.14
6	Ni _{0.75} Ti _{0.25} O	3.73	1.42
7	Ni _{0.70} Ti _{0.30} O	3.48	1.71

b) Sol-gel solution for NiO co-doped with Ti and Sn (NiO:Ti:Sn) films

Tin dopant was added in order to compensate Ti matrix in the NiO amorphous structure. After annealing the films, the structure formula is

assumed to be “Ni_{1-x}Ti_{x-y}Sn_yO” as assumed by Dae-hoon park for Zn dopant that compensate Ti in the NiO:Ti films [25].

For the films of NiO doped with Ti alone (previously prepared), the best sample, in term of electrochromic properties, was found for the NiO films that contains molar concentration ratio of 0.25 of Ti (Ni_{0.75}Ti_{0.25}O). Hence for the NiO co-doped with Ti and Sn, we will maintain the Ni molar concentration ration to 0.75; Sn will compensate Ti species only. Accordingly, the structure formula can be written as “Ni_{0.75}Ti_{0.25-y}Sn_yO”.

0.5 M sol-gel solution of Ni_{0.75}Ti_{0.25-y}Sn_yO was prepared in 40 ml ethanol; with Sn molar concentration varies from 0.0 - 0.25 (see table 3.2). The sol-gel was prepared by adding SnCl₂.2H₂O to 40 ml of ethanol and stirred by magnet for at least 6 hours (transparent colorless solution was obtained). Ti-isopropoxide was then added to the mixture to be mixed on the stirrer for 30 min. Finally, Ni(CH₃COO)₂.4(H₂O) was added to the mixture, which is left to be magnetically stirred (2 hours at least) until it was totally dissolved (a transparent green colored was obtained).

Table (3.2): list of intended composition, Ti-isopropoxide mass, and tin (II) chloride mass used in the sol-gel preparation. All sol-gel solutions contain 3.73 gm of Nickel acetate and they were prepared in ethanol total volume of 40 ml.

Sample no.	composition	Ti-isopropoxide (gm)	Tin (II) chloride (gm)
1	Ni _{0.75} Ti _{0.25} O	1.42	0.00
2	Ni _{0.75} Ti _{0.24} Sn _{0.01} O	1.36	0.05
3	Ni _{0.75} Ti _{0.23} Sn _{0.02} O	1.31	0.09
4	Ni _{0.75} Ti _{0.22} Sn _{0.03} O	1.25	0.14
5	Ni _{0.75} Ti _{0.21} Sn _{0.04} O	1.19	0.18
6	Ni _{0.75} Ti _{0.20} Sn _{0.05} O	1.14	0.23
7	Ni _{0.75} Ti _{0.10} Sn _{0.15} O	0.57	0.68
8	Ni _{0.75} Sn _{0.25} O	0.00	1.13

3.2 Measurements

3.2.1 Cyclic voltammetry (CV)

Cyclic voltammetry is a technique in which the potential of the working electrode against the reference is swept periodically and linearly between two fixed values at a certain scan rate and the current flow between the working electrode and the counter electrode is recorded. This has the advantage that the product of the ion and electron transfer reaction that occurred in the forward scan can be probed again in the reverse scan.

The cyclic voltammetry experiments were performed using one compartment three electrodes electrochemical cell which presented in Fig. 3.2, that contains 0.5 M KOH aqueous solution as an electrolyte. The NiO-based electrochemical films deposited on FTO/Glass were used as working electrode (WE), the silver/silver chloride (Ag/AgCl) was used in the cell as reference electrode (RE), and the platinum was used as counter electrode (CE).

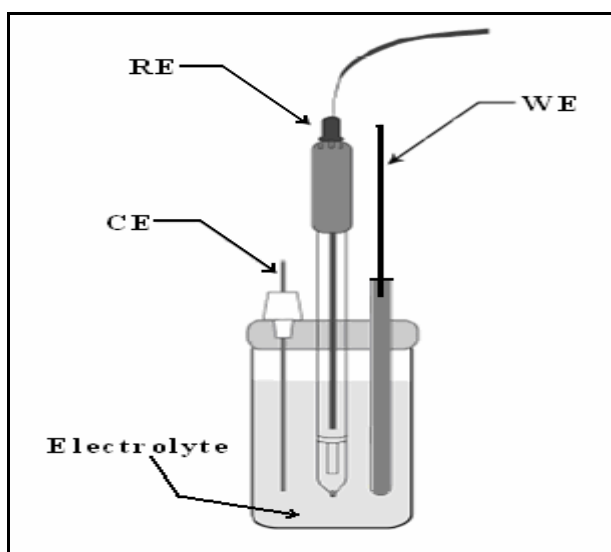


Fig. (3.2): A schematic shows one compartment three electrodes electrochemical cell

a)NiO:Ti films

CV (cyclic voltammetry) measurements were done, at room temperature, using a radiometer Polarograph MDE 150 coupled with polarographic analyser POL 150. The potential varied between -0.65 V and 0.65 V, versus Ag/AgCl reference electrode, at a scan rate of 10 mV/s. The potential cycles varied between 1 and 30 cycles for each electrochromic film. In order not to exceed the upper limit of current (1 mA only) of the polarograph, the film area which was immersed in the electrolyte was kept $\sim 0.4 \text{ cm}^2$.

b)NiO:Ti:Sn films

To enhance the current scale, CV measurements were performed, at room temperature, using Princeton Applied Research PAR 263A Potentiostat/Galvanostat. The film area immersed in the electrolyte was $\sim 2 \text{ cm}^2$. CV experiment conditions was like those performed for NiO:Ti films; The potential varied between -0.65 V and 0.65 V, versus Ag/AgCl reference electrode, at a scan rate of 10 mV/s, and the potential cycles varied between 1 and 30 cycles for each electrochromic film.

3.2.2 Transmittance

The transmission of light using varied or single wavelength was performed using Shimadzu UV-3101PC UV-Vis-NIR scanning spectrophotometer. The transmittance of the NiO-based electrochromic films was performed at wavelength varied from 290 – 800 nm. Also, the

transmittance of glass and FTO/glass substrate was performed for reference spectra. Moreover, the transmittance, of different NiO-based electrochromic films, during CV measurements (coloring and bleaching), was performed at a wavelength of 550 nm.

3.2.3 Photoluminescence (PL) measurements

A perkin-Elmer LS 50 luminescence spectrophotometer was used to measure solid state emission fluorescence spectra for different NiO-based film samples. Emission spectra were used to estimate the band gap of the electrochromic films, where $E_{\text{gap}}=1240/\lambda_{\text{emi}}$. The optimized composition “Ni_{0.75}Ti_{0.22}Sn_{0.03}O” was used for photoluminescence experiment. We have used films of two and three time dipping on glass to have more thick material in order to obtain rather good PL results. The emission spectra for the film were collected from 200-800 nm. The excitation wavelengths of 307 nm was chosen from scanned excitation spectra (from 200-800 nm) that was performed for the NiO:Ti:Sn/Glass film. Also, the emission spectra for glass at the same excitation wavelengths were also performed for reference spectra.

3.2.4.X-Ray Diffraction (XRD)

The x-ray diffractometer analyze crystalline states under normal atmospheric conditions. In this method, x-rays focused on a sample, fixed on the rotating axis of the spectrometer (goniometer), are diffracted by the sample. The changes in the diffracted x-ray intensities at different angles

are measured, recorded and plotted against the rotation angles of the sample. The result is referred to as the XRD of the sample. Qualitative analysis may be conducted on the basis of peak height or peak area. The peak angles and profiles may be used to determine particle diameters and degree of crystallization, and are useful in conducting precise x-ray structural analysis using computerized analysis methods.

XRD For NiO-based electrochromic films were recorded on a philips X'PERT PRO X-Ray diffractometer equipped with $\text{CuK}\alpha$ radiation ($\lambda=1.5418 \text{ \AA}$) as a source. The spectra were kindly recoded at ICMCB-CNRS, University of Bordeaux I, Bordeaux, France.

XRD was performed for NiO-based electrochromic films on FTO/glass substrates. The detector angle (2θ) varies between 8° and 80° in steps of 0.02° . XRD measurements were also repeated for the same samples for prolonged time (~ 50 times higher for given angle); the detector angle (2θ) ranges between 35° and 45° in steps of 0.017° , where highest peak intensity of NiO exist.

3.2.5 Scanning Electron Microscopy (SEM)

Field emission scanning electron microscopic / energy dispersive spectroscopic (FE-SEM/ EDS) studies were conducted on a Joel microscope, model JSM-6700F, at CREMEM - University of Bordeaux.

SEM is useful to directly study the surfaces of solid objects. By scanning with an electron beam that is generated and focused by the

operation of the microscope, SEM uses electrons instead of light to form an image. A beam of electrons is produced at the top of the microscope by heating of a metallic filament. The electron beam follows a vertical path through the column of the microscope. It makes its way through electromagnetic lenses which focus and direct the beam down towards the sample. Once it hits the sample, other electrons are ejected from the sample. Detectors collect the secondary or backscattered electrons, and convert them into a signal that is sent to a viewing screen to produce an image.

Chapter Four

Results and Discussion

Chapter Four

Results and Discussion

Nano-particles of NiO semiconducting electrochromic thin films, doped by Ti and/or Sn, have been prepared. The effects of doping and co-doping, on prepared films characteristics (electrochromic, optical, and structural), have been studied using different measuring techniques listed below:

- 1- Cyclic Voltammetry (CV).
- 2- Photoluminescence Spectra.
- 3- Optical transmission Spectra.
- 4- X-Ray Diffraction Technique (XRD).
- 5- Scanning Electron Microscopy Images (SEM).

4.1 Nickel oxide doped with Titanium (NiO:Ti) thin films

In previous studies, nickel oxide showed poor electrochromic properties when cycled in KOH or other electrolytes; low cycling durability, permanent brown color after about 50 cycles, and was easily degraded [17, 20- 21]. However, doping NiO with various dopants was found to highly enhance electrochromic, structure, durability, and adhesion to substrate [22,96-97, 23].

0.5 M sol-gel solution of $\text{Ni}_{1-x}\text{Ti}_x\text{O}$ was prepared in our lab (see section 3.1.3-a) under ambient conditions. It was observed that the prepared

solution was ambiguous and not transparent with light green color. This is due to the hydrolysis of Ti-isopropoxide in mixture when prepared under ambient condition. This was also observed by A. Alkahlout when NiO:Ti [31] according to this, she prepared the NiO:Ti solution and dipped the films in the dry glove box, when using Ti-isopropoxide .

NiO:Ti electrochromic nano-particles films have been prepared onto FTO/glass substrate. Double layer of NiO:Ti was prepared by dipping the substrates in the prepared sol-gel solutions for two times. After dipping, the films were annealed at 350° for 1.5-2 hours.

4.1.1: Cyclic Voltammetry (CV)

Cyclic voltammograms was measured, during 30 cycles, for NiO:Ti in 0.5 M KOH electrolyte. The potential was cycled between -0.65 and 0.65 V, versus Ag/AgCl reference electrode, at a scan rate of 10 mV/s [25, 31, 32]. CV experiments have been performed for prepared NiO films doped with different Ti concentrations ($\text{Ni}_{1-x}\text{Ti}_x\text{O}$). The concentrations varied from 0-30 % in steps of 5 % (Figure 4.1).

As we can noticed from CV measurements which were registered in our lab, no electrochemical, and hence no electrochromic, activity are observed in the anodic potential range -0.6 to an average (for all films) of about -0.1 V. Anodic current density (+J), associated with the coloration of the electrochromic layer, start to be more pronounced at anodic potential higher than 0.2 V. For anodic potential higher than about 0.4V , the anodic

current density sharply increases until reaching its peak at about 0.5 V for NiO and ranges from 0.55-0.65 V for NiO:Ti films. For each CV measurement, the anodic current density peaks was found to slightly shift to higher potential with increasing number of cycles. The other raise in the anodic current density for potential between 0.6 and 0.65 V is due to oxygen evolution in the electrochemical reaction [98]. A single cathodic current density peak associated with the film bleaching is observed at about 0.37 V for NiO and reduces to about 0.3 for NiO:Ti films. For some films, the cathodic peaks are also observed to be slightly shifted towards lower or higher potential values.

As we can observe, there is an increase in anodic peak positions, and decrease cathodic peak positions for NiO:Ti films compared to NiO film. This may be attributed to the structure modifications or existence of more than one phase (as will be seen later from XRD) associated with Ti dopings. Also, for a given CV measurement, the slight shift in the peaks position, for the anodic and cathodic current density, could be attributed to the natural difference in the hydroxide/oxyhydroxide phases upon cycling [36, 34, 89].

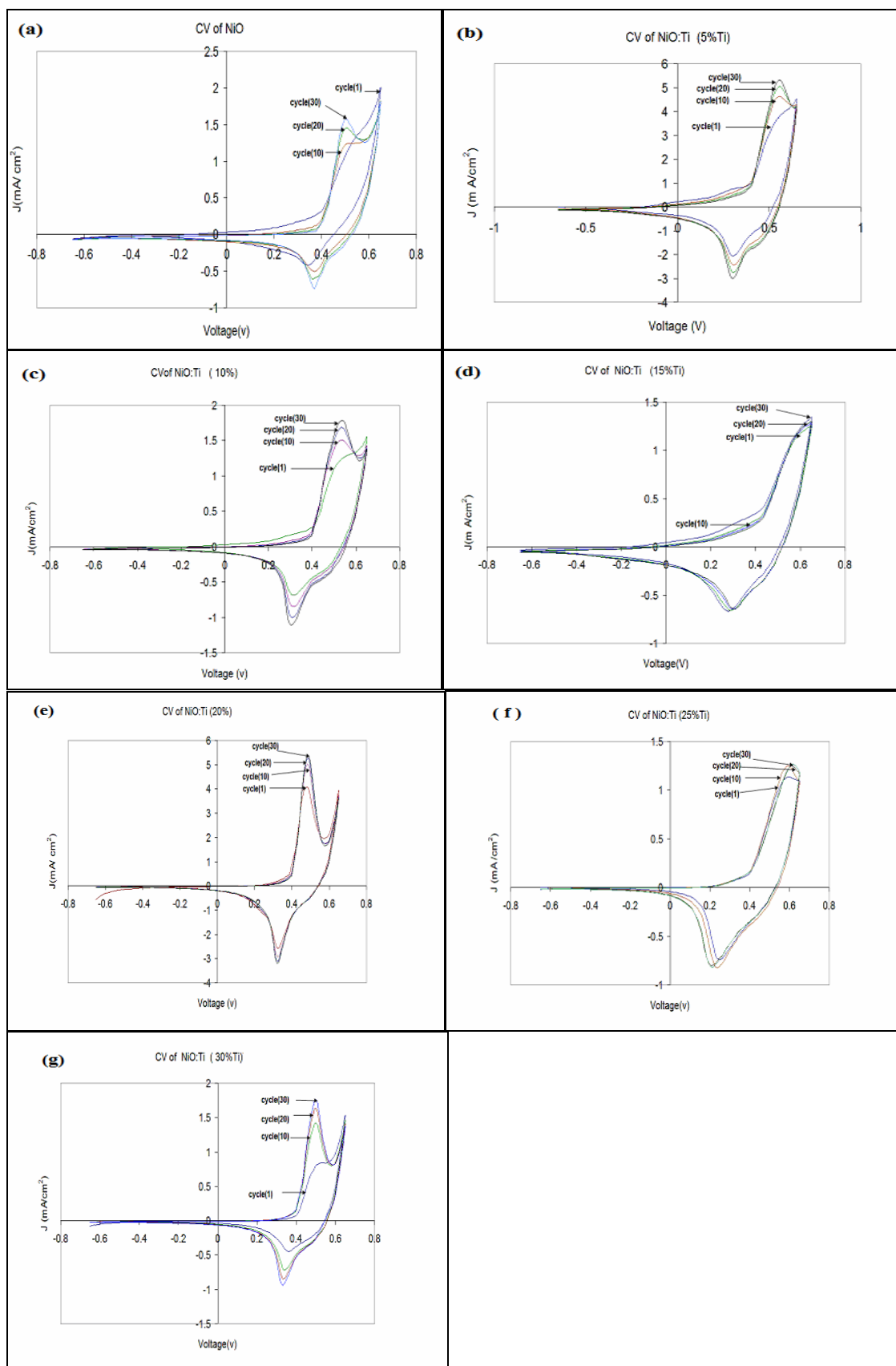


Fig. (4.1): Cyclic voltammety measurements for cycles no 1,10, 20, and 30 for NiO:Ti with different Ti molar concentrations: a) NiO, b) $\text{Ni}_{0.95}\text{Ti}_{0.05}\text{O}$, c) $\text{Ni}_{0.9}\text{Ti}_{0.1}\text{O}$, d) $\text{Ni}_{0.85}\text{Ti}_{0.15}\text{O}$, e) $\text{Ni}_{0.8}\text{Ti}_{0.2}\text{O}$, f) $\text{Ni}_{0.75}\text{Ti}_{0.25}\text{O}$, and g) $\text{Ni}_{0.7}\text{Ti}_{0.3}\text{O}$.

The current density(J) in the CV measurements is plotted versus time t (Fig. 4.2), it is can be deduced that anodic (Q_a) and cathodic charge density (Q_c); Q_a is the charge associated with anodic current density ($+J$) and Q_c is the current density related to the cathodic current density ($-J$). Indeed, Q_a can be deduce by integrating the J - t graphs according to

$$Q = A \int J dt \quad (4.1)$$

The anodic current density ($+J$) peak is observed to increase with increasing number of cycles (can be observed also from CV measurments of Fig. 4.1). This indicate an increase in the anodic charge density Q_a injected in the layer during coloration of the layer. However, it is not obvious that the calculated Q_a will increase with cycle number. This behavior was assigned to oxygen evolution that is related to the second observed anodic peak at $t = 130$ s (for potntial of 0.65V) [98]. The oxygen evolution current density was found to be more pronounced for NiO film. This may be attributed to the anodic current density peak position that have lower anodic potential (0.5V) than NiO:Ti ($> 0.5V$) films.

The cathodic current density ($-J$) was also observed to increase with increasing number of cycles. This indicates that increase in the cathodic charge density Q_c is extracted from the layer during the bleaching process (change from full coloration to full transparent). In order to exclude the influence of the oxygen evolution, we can depend on Q_c for calculating the charge density needed for coloration or bleaching of the layer.

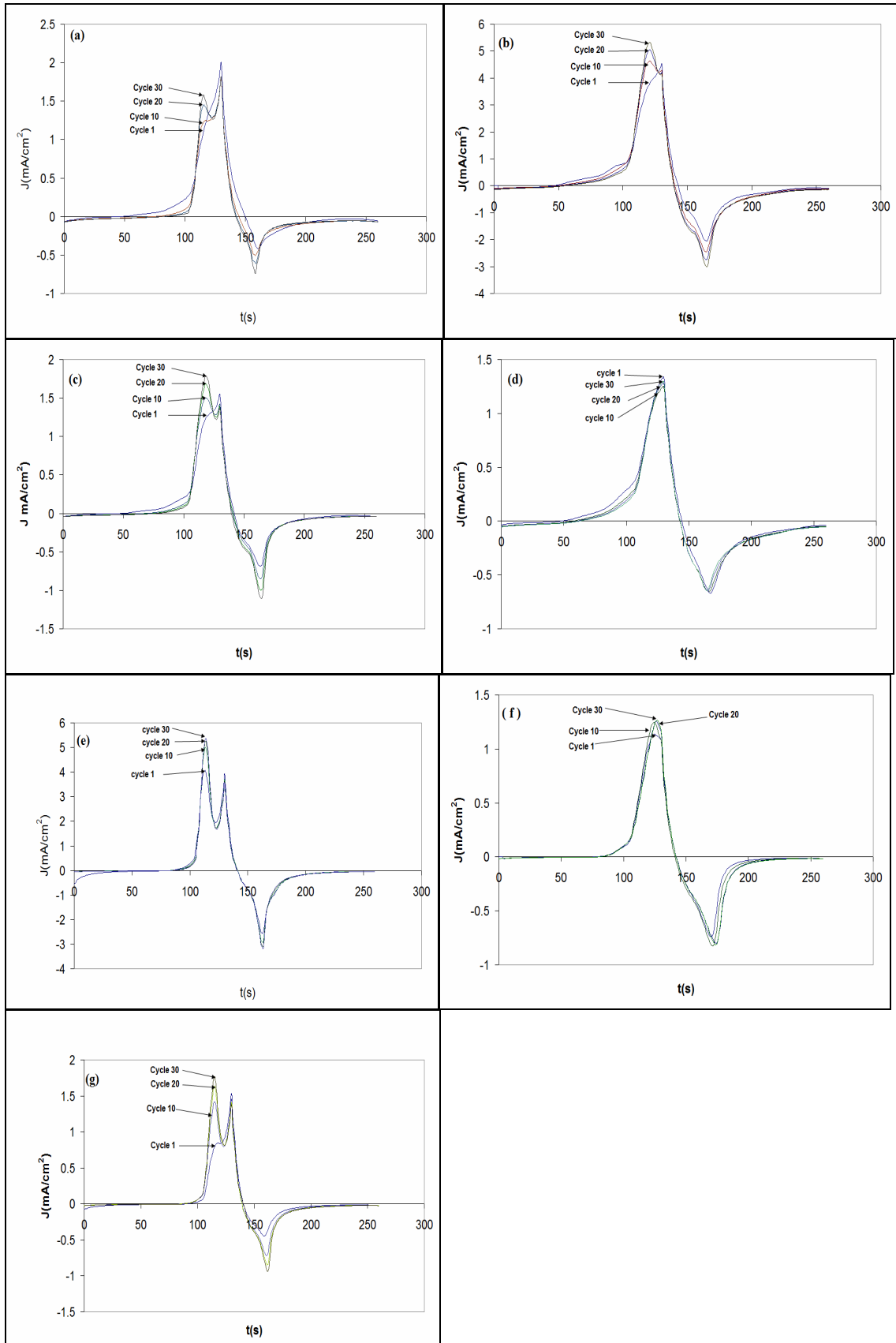


Fig. (4.2): Current density with time for cycles no 1,10, 20, and 30 for $\text{NiO}:\text{Ti}$ with different Ti molar concentrations: a) NiO , b) $\text{Ni}_{0.95}\text{Ti}_{0.05}\text{O}$, c) $\text{Ni}_{0.9}\text{Ti}_{0.1}\text{O}$, d) $\text{Ni}_{0.85}\text{Ti}_{0.15}\text{O}$, e) $\text{Ni}_{0.8}\text{Ti}_{0.2}\text{O}$, f) $\text{Ni}_{0.75}\text{Ti}_{0.25}\text{O}$, and g) $\text{Ni}_{0.7}\text{Ti}_{0.3}\text{O}$.

Ideally, for a given CV cycle, Q_a and Q_c should be equal ($Q_a/Q_c = 1$) for a full reversible electrochromic process and with no oxygen evolution. Practically, even for high reversible electrochromic devices with no oxygen evolution, Q_a is always higher than Q_c . This is due to the fact that there is almost a continuous change in the hydroxide/oxihydroxide nature during cycling process, freshly precipitated insulating $Ni(OH)_2$ particles by KOH, and wetting of the layer from KOH electrolyte [98, 25, 31, 32, 80]. Indeed, this will affect the transparency of the electrochromic layer for both coloration and bleaching states. The calculated Q_a , Q_c and Q_a/Q_c for cycled NiO:Ti films are shown in table 4.1.

Table (4.1): calculated Q_a , Q_c and Q_a/Q_c for cycles 1, 10, 20, and 30 of NiO doped with different molar concentration of Ti.

Sample composition	Cycle number	Q_a (mC)	Q_c (mC)	Q_a/Q_c
NiO	1	46.14	13.44	3.43
	10	37.54	17.01	2.20
	20	37.87	18.20	2.08
	30	37.79	18.59	2.03
Ni_{0.95}Ti_{0.05}O	1	121.29	66.47	1.82
	10	123.59	82.14	1.50
	20	122.49	90.64	1.35
	30	122.98	95.62	1.29
Ni_{0.9}Ti_{0.10}O	1	37.46	19.20	1.95
	10	37.09	22.90	1.61
	20	37.64	24.87	1.51
	30	37.74	26.97	1.39
Ni_{0.85}Ti_{0.15}O	1	36.21	24.69	1.46
	10	31.54	27.20	1.15
	20	31.17	27.04	1.15
	30	30.80	27.04	1.13
Ni_{0.8}Ti_{0.20}O	1	86.52	46.65	1.85
	10	87.86	57.99	1.51
	20	88.11	59.20	1.48
	30	87.70	59.29	1.47
Ni_{0.75}Ti_{0.25}O	1	25.99	18.12	1.43
	10	26.86	21.53	1.24
	20	26.34	22.32	1.18
	30	26.27	22.63	1.16
Ni_{0.7}Ti_{0.30}O	1	25.41	12.91	1.96
	10	29.92	17.12	1.74
	20	31.41	19.21	1.63
	30	32.35	20.14	1.60

As expected, the calculated Q_a was found to have no regular tendency with increasing number of cycles. On the other hand, Q_c always increases with increasing cycles. The increase in the current density with cycles number of indicates that the amount of coloring sites available for the redox reaction increases and did not reach the limit of saturation yet

[32]. It was reported by different researchers [32, 99, 80], that charge density increases to a certain number of cycles (couple of hundreds) and then saturates at higher number of cycles (may reach thousands). After that, it is reduced due to the decomposition of the electrochromic layer or dissolution of the NiOOH phase structure [17].

The ration Q_a/Q_c is found to be higher than one and reaches an average of about 2.5 for NiO cycled film. For NiO:Ti cycled films, the ration reaches an average of about 1.5 or even less. This indicates that the NiO:Ti films have better electrochromic properties in term of reversibility and less oxygen evolution than NiO film. The reason for this may be due to the dependence of anod current on applied potential. The higher the point, the higher the anodic current. The ratio Q_a/Q_c for NiO:Ti with titanium contents of 15% and 25% are found to approach 1 (about an average of about 1.2 for both). In fact, this is expected because if we look to figure 4.1 or figure 4.2, we can observe that the anodic peak current is shifted to the higher anodic potential value. Hence this in turn will reduce the current peak for oxygen evolution in the electrochemical reaction. Hence, we can conclude that these films have the best electrochromic properties in term of reversibility.

4.1.2 Optical properties

a) Transparency

In addition to reversibility, Color change in the visible light is one important feature of electrochromic devices; the more increase in the

transmission contrast ration between coloration and bleaching (T_b/T_c) of the electrochromic film, the more efficient the electrochromic device.

For reference purposes, the transmission for the glass and FTO/glass substrates were scanned, in the visible range, at a wavelength varied from 290-800 nm. They were scanned against air as a reference. The transmission of light during CV measurements (coloring and bleaching), was carried out at a wavelength of 550 nm for the cycle number 29 and 30. The wavelength of 550 nm was chosen because it represents the maximum luminous sensitivity for human eye [100]. The measurements were carried out for the layers in the three electrode electrochemical cell , at normal incident angle and against a reference cell that contains 0.5 M KOH. Also, the transmittance during CV was always reset to 100 % before running each experiment.

Figure 4.3 showed the transparency spectra for glass and FTO/glass substrate. The glass was found to have a high transparency, in the visible range, of an average value of about 91 % with respect to air. FTO/glass substrate showed a relatively high transparency, in the visible, with an average of 80 % with respect to air and 88 % with respect to glass. At a wavelength of 550 nm, the transparency of FTO with respect to air reaches 80 %. The fringes which appeared transmittivity in substrate are due to the thickness of FTO film on glass. This is due to the fact that FTO have a large energy band gap (~ 3.6 eV) [40].

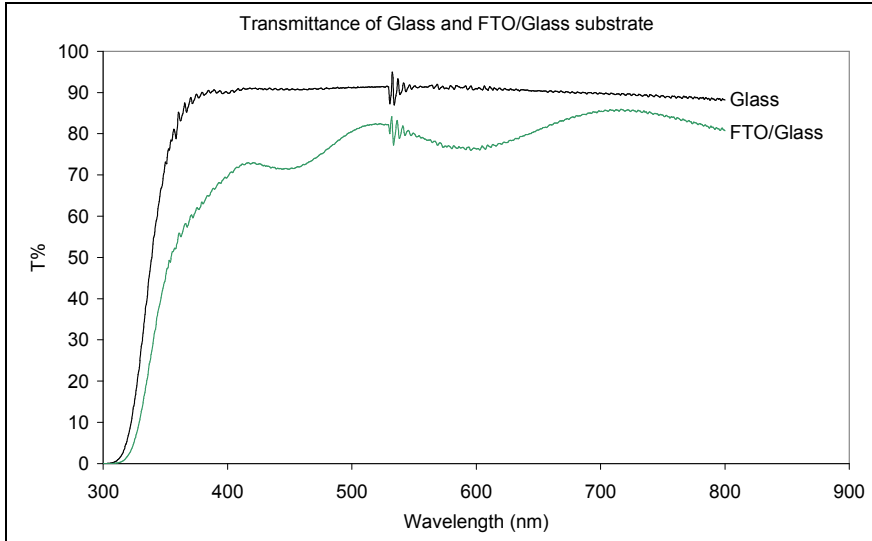


Fig. (4.3): Visible range Transparency (T) spectra for glass and FTO/glass substrate; air is set as a reference.

The transparency spectra, at 550 nm, for coloration and bleaching (during CV measurements) of NiO:Ti electrochromic films, with different Ti molar concentrations, are presented in figure 4.4.

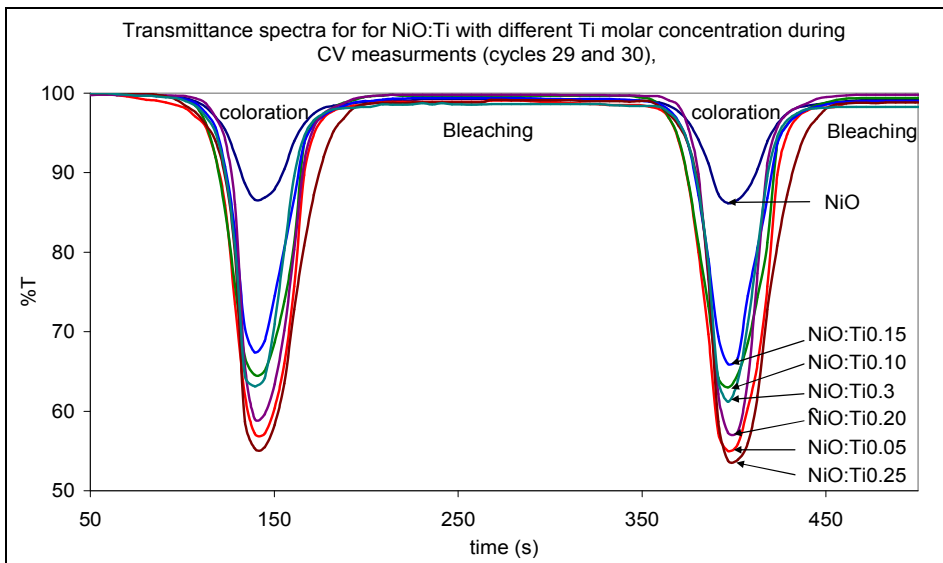


Fig. (4.4): Coloration and bleaching transparency (T) spectra, during CV measurements (cycles 29 & 30), for double layer NiO:Ti with different Ti molar concentrations.

All films showed a high transparency during bleaching process. However, the transparency in the bleaching process (T_b) slightly decreases with cycling. This is, as quoted above, due to wetting of the layer and

freshly precipitated $\text{Ni}(\text{OH})_2$ [98, 25, 31, 32, 80]. On the other hand, The transparency during coloration state (T_c) for $\text{NiO}:\text{Ti}$ films was found to be lower than NiO film. It was also observed that T_c differs, without regular tendency, for different Ti molar concentrations. Also, as we can observe, T_c slightly decrease with increasing cycle number. The decrease of T_c with cycles indicates that the amount of coloring sites available for the redox reaction increases and not reaches saturation yet [32]. The lowest T_c ($\sim 54\%$) was observed, in the figure, for the film doped with 25% of Ti ($\text{NiO}:\text{Ti}_{0.25}$).

Indeed, the coloration of the film during CV measurements is associated with anodic current density (+J). Also, the bleaching process is associated with the cathodic current density (-J). This claim can be observed from figure 4.5, in which we plot both transparency and current density during CV measurement (cycle 30) for the $\text{NiO}:\text{Ti}_{0.25}$ electrochromic layer.

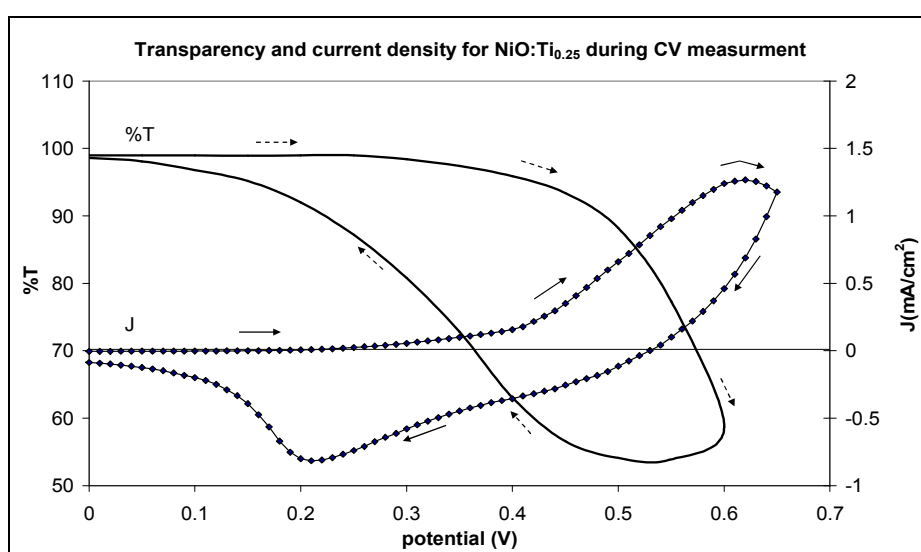


Fig. (4.5): Transparency and current evolution during CV measurement for $\text{NiO}:\text{Ti}_{0.25}$ layer. (\rightarrow) indicates the current evolution and ($- - - \rightarrow$) indicates corresponding Transparency evolution.

The figure showed that the coloration of the layer (transparency reduces) takes place at the beginning of the anodic current (+J). The transparency reaches its minimum value (T_c) at the instant the current density reaches zero value (the end of anodic current). The bleaching of the layer (transparency increases) is observed during the cathodic current (-J). the value of transparency reaches its maximum again (T_b) when -J reaches about zero value again. Therefore, as mentioned before, since the cathodic current is the current for a complete change between coloration and transparency, we can use it to calculate the charge (Q_c) needed to color the layer. the anodic current is not used in calculation due to the probability of oxygen evolution during coloration of the layer.

For the different NiO:Ti films, figure 4.4 and Q_c for cycle 30 from table 4.1 was used to calculate the contrast ratio (T_b/T_c) and coloration efficiency (CE). The calculated quantities (T_b/T_c and CE) are then tabulated in table 4.2.

Table (4.2): calculated contrast ration (T_b/T_c) and coloration efficiency (CE) for cycle 30 of NiO films doped with different molar concentration of Ti.

Sample composition	Q_c (mC/cm ²) for cycle 30	T_b	T_c	T_b/T_c	CE(cm ² /C)
NiO	18.59	99.10	86.58	1.14	3.2
Ni _{0.95} Ti _{0.05} O	95.62	98.81	55.00	1.80	2.7
Ni _{0.90} Ti _{0.10} O	26.97	99.41	63.10	1.58	7.3
Ni _{0.85} Ti _{0.15} O	27.04	98.99	68.26	1.45	6.0
Ni _{0.80} Ti _{0.20} O	59.29	98.50	56.00	1.76	4.1
Ni _{0.75} Ti _{0.25} O	22.63	98.81	53.83	1.84	11.7
Ni _{0.70} Ti _{0.30} O	20.14	98.28	62.17	1.58	9.9

As observed for T_c before, no regular tendency was observed for T_b/T_c and CE with increasing Ti concentration. But, almost all NiO:Ti electrochromic layers showed higher T_b/T_c and CE than NiO film. NiO films is known to have low cycling life, low reversible properties (transparency in the bleach state rapidly decrease upon cycling), and very poor adhesion to the substrate [17, 20 - 21]. On the other hand, doping NiO with Ti highly enhances the electrochromic properties due to the improvement of adherence, scratch resistance, stability (reversibility), and transparency of the films in their bleached state[25, 32].

Also from table 4.2, The layer with the best T_b/T_c and CE is the one that have Ti molar concentration of 25% (NiO:Ti_{0.25}). This composition was also found to have a high reversibility (Q_a/Q_c approaches 1) and was expected to have the highest electrochromic properties (see section 4.1.1). This may be attributed to the fact that 25% of Ti represents the solubility limit of titanium dopant within the NiO matrix, as will be shown later by XRD measurements (section 4.1.3). Confirming our findings, this composition prepared and tested under different condition by A. alkahlout [31, 32] was found also to have best electrochromic properties.

b) Photoluminescence (PL)

The high transparency, in the visible light region, observed for bleached state of NiO based electrochromic film is due to fact that they have a rather high energy band gap ($> 3eV$). This will reduce absorption in the visible range and make the material transparent. PL emission spectrum

was done for as prepared NiO:Ti_{0.25} electrochromic films (transparent bleach state), deposited on glass substrates (figure 4.6). UV excitation wavelength ($\lambda_{\text{ext}} = 307 \text{ nm}$) was used to excite the electrons from the material valence band. For substrate reference, PL emission spectrum for glass was also performed (presented on same figure).

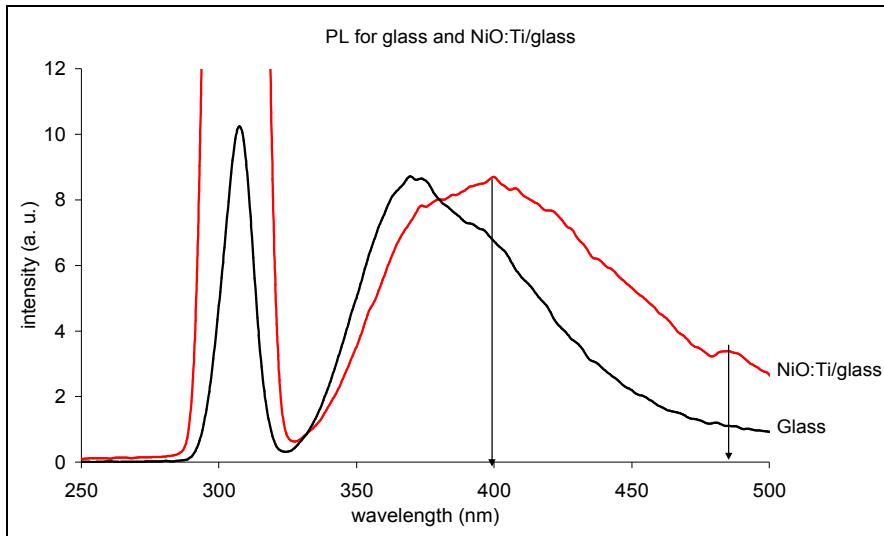


Fig. (4.6): Photoluminescence spectra for glass and NiO:Ti/glass

Compared to glass substrate, a widening for the PL broad peak was observed for NiO:Ti/glass sample with maximum intensity at about $\lambda = 400 \text{ nm}$. This peak is clearly related to NiO:Ti layer band gap transition. The band gap, E_g , for the layer is estimated to have a value of 3.10 eV ($E = hc/\lambda = 1240 \text{ eV.nm}/400 \text{ nm}$). Estimated E_g value indicates that our film is transparent in the visible light region. This is in full agreement with other researchers [99-100] who found E_g for NiO based thin films to have a value ranges between 3-4 eV. Other peak is also observed at wavelength of about 485 nm ($E = 2.56 \text{ eV}$). It may correspond to inter band transitions (surface energy states) due to defects such as oxygen vacancies, Ni interstitials, or other impurities in addition to incomplete bonding.

Indeed, other excitation wavelengths were used for PL spectra. They were chosen from a full range scanning excitation wavelengths (Figure 4.7). Most of tested excitation wavelength showed no clear discrepancy between glass and NiO:Ti film; it is probably that PL spectrum for NiO:Ti is screened by glass PL spectrum. Hence, they are not presented because they have no reliable results.

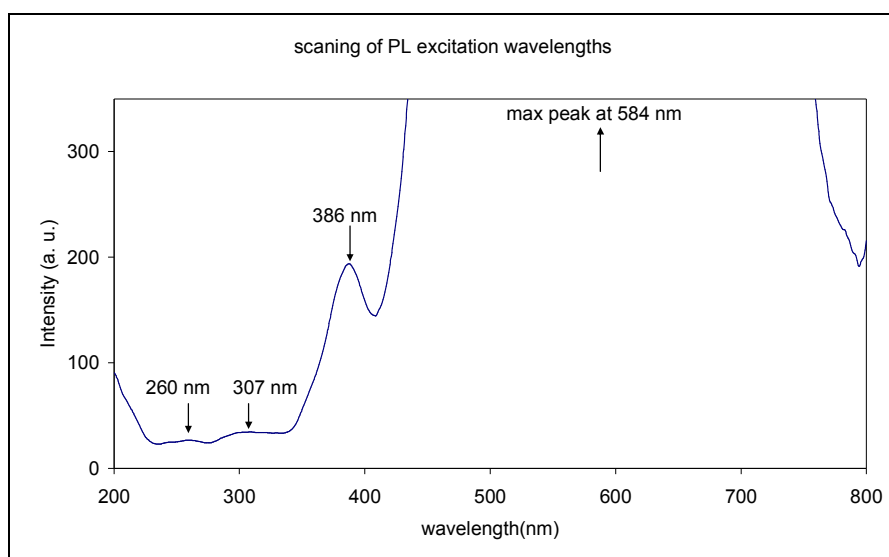


Fig. (4.7): Scanning for PL excitation wavelengths.

4.1.3: Structural properties

a) X-Ray diffraction (XRD):

XRD patterns for prepared NiO:Ti with different Ti molar concentration (0%, 10%, 20%, and 30%) is presented in Figure 4.8. For all NiO-based films with different Ti molar concentration, no peaks corresponds to NiO phase (JCPDS reference pattern 078-0429) was detected. To be sure of this result, XRD for NiO:Ti films was done for prolong time between 35 and 45° (figure 4.9) . This angle range was chosen

because it includes the highest intensity peaks of preferential orientations (111) and (200). Also no peaks corresponds to NiO phase was detected. This proved that the NiO-based thin films were probably amorphous in structure, with no preferable orientation. Amorphous structure for NiO-based films was also obtained, with an average crystallite size between 3-7 nm, when prepared by dipping in a sol-gel solution and annealed up to 350 °C [10, 25, 32]. They observed a crystallite size smaller than that published for pure NiO films prepared by sputtering, 20 to 300 nm [103] and sol-gel, 8 to 150 nm [21]. Hence, it is known that the presence of Ti dopant decreases the growth of the NiO crystallites. Consequently, higher surface area of the film will be exposed to electrochemical reaction. This may have a role for the better electrochromic properties for amorphous NiO:Ti phase with lower grain size.

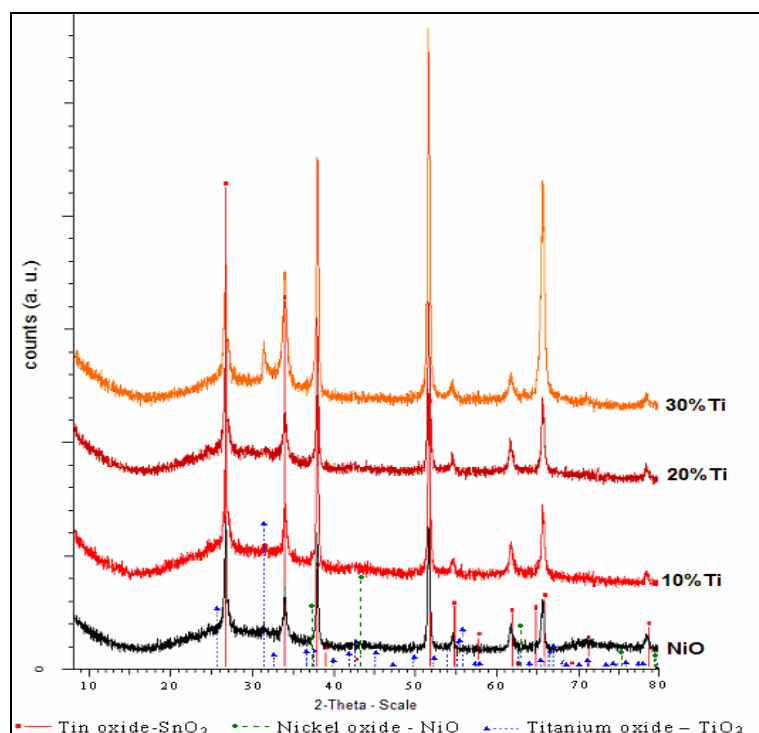


Fig. (4.8): XRD pattern for NiO:Ti with different Ti molar concentration. SnO₂, NiO, and TiO₂ reference patterns are shown in the figure.

Most of the peaks observed in the XRD patterns are related to the well crystallized FTO film (JCPDS reference pattern 088-0287 for SnO₂) that deposited on glass substrate. Only one peak that may corresponds to TiO₂ (JCPDS reference pattern 084-1750) could be detected for NiO:Ti film with Ti molar contents of 30%. This indicates that the molar solubility limit of TiO₂ within the NiO structure is between 20 and 30%. This may describe the best electrochromic results observed for NiO doped with 25% of Ti (NiO:Ti_{0.25}). For higher doping concentrations (Ti concentration 30% or higher), compositional inhomogeneity and disorder structure due to TiO₂ phase may introduced in the NiO film. This in turn negatively affects the electrochromic properties of the film.

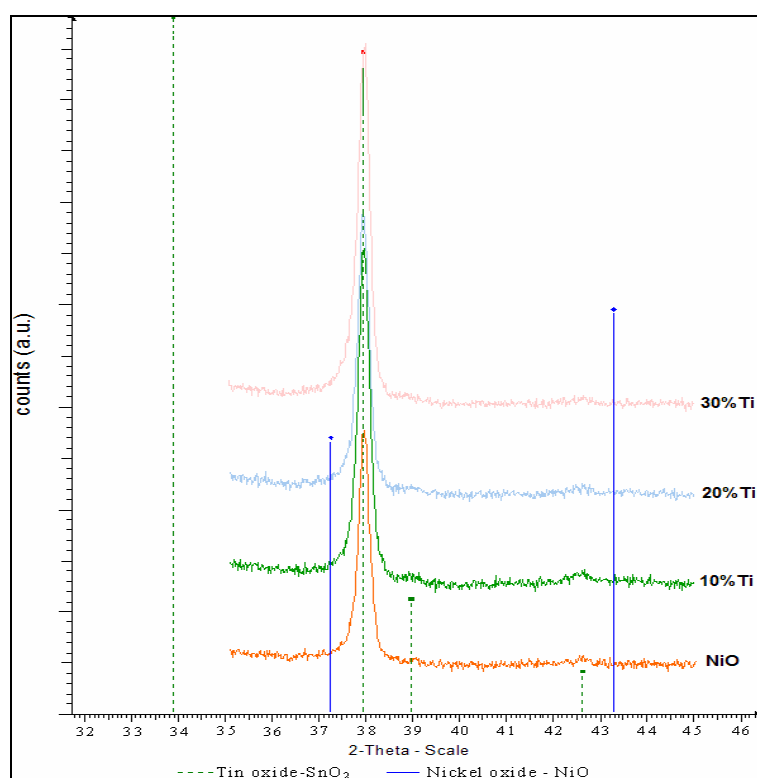


Fig. (4.9): Prolong time XRD pattern for NiO:Ti with different Ti molar concentration. SnO₂, and NiO reference patterns shown on the figure.

b) Scanning Electron Microscopy (SEM):

In order to study the morphology of the prepared films, highly magnified FE-SEM images (figure 4.10) have been done for surfaces of NiO-based films doped with 10% and 20% of Ti.

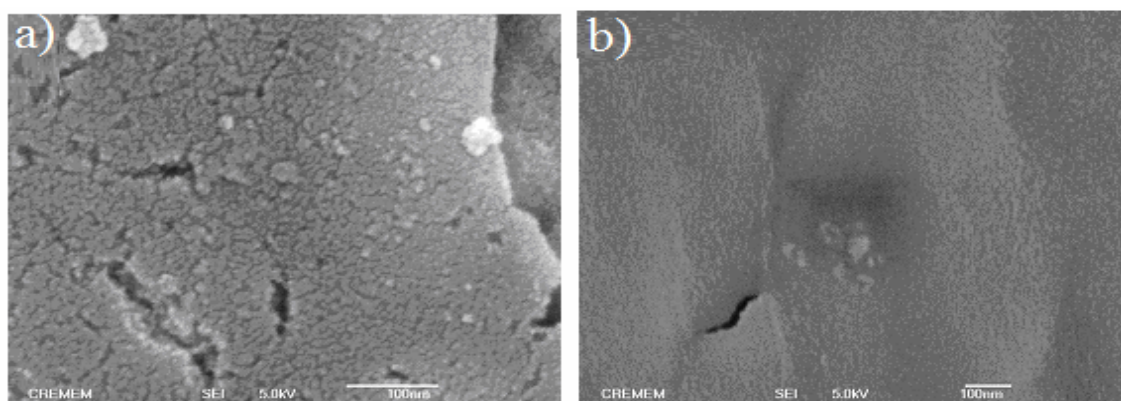


Fig. (4.10): FE-SEM for NiO:Ti films with Ti molar concentration a) 10% and b) 20%.

For both compositions, the figure reveals the amorphous structure of the films. The observed amorphous morphology, for the films, confirms the results obtained from XRD measurements where we found no peaks correspond to NiO phase. Similar surface morphology was observed for amorphous films prepared by sol-gel using spin coating deposition method [25].

Film with 20% of Ti showed a higher homogeneity surface with less cracks than the one of 10% of Ti. The cracks or voids observed in both films may due to annealing of the film at high temperature (350 °C). Hence, increasing the Ti dopant molar concentration within NiO matrix increases the homogeneity of the film. Further, the higher the temperature the more probable the surface oxidation.

A grain size varies from 6-17 nm for a film contains 10% of Ti. For films of 20% of Ti, the grain size ranges from 3-9 nm in diameter. As a result, doping with higher concentration of Ti decreases the NiO-based film crystallite size. Consequently, higher surface area will be exposed to the electrochemical reaction, and hence higher coloration. This confirms findings of other researchers [103, 21], where they found better electrochromic properties for less crystallite size films was reported.

4.1.4 Conclusions

Despite the hydrolysis occurs when preparing the sol-gel solution, the cycle stability, reversibility, and coloration efficiency of the NiO films are improved upon doping with Ti. This is attributed to better adherence and scratch resistance. Due to its higher homogeneity and less grain size, best electrochromic properties were observed for films doped with 25% Ti (which show best CV and transmittance results). Less homogeneous films with higher grain size was observed for lower dopant ratio. However, for higher dopant ratios (> 25 mol. % of Ti), TiO_2 phase was observed, which may cause a compositional inhomogeneity and disordered film structure, which negatively affected the electrochromic properties.

4.2 Nickel oxide co-doped with Ti and Sn (NiO:Ti:Sn) thin films

Doping NiO with 25 mol. % of Ti was found to highly enhance the electrochromic properties in KOH electrolyte. However, co-doped NiO with Ti and Zn dramatically increase the electrochromic properties by increasing electrochromic durability for the films upon cycling [25].

Following same strategy, NiO doped with both Ti and Sn electrochromic nano-particles films have been prepared onto FTO/glass. For the films of NiO doped with Ti alone, the best sample, in term of electrochromic properties, was found for the NiO films that contains molar concentration ratio of 0.25 of Ti ($\text{Ni}_{0.75}\text{Ti}_{0.25}\text{O}$). Hence, for the NiO co-doped with Ti and Sn, we will maintain the Ni molar concentration ration to 0.75; Sn will compensate Ti species only, as assumed by D. Park [25] for Zn dopant that compensate Ti in the NiO:Ti films. Accordingly, the structure formula can be written as " $\text{Ni}_{0.75}\text{Ti}_{0.25-y}\text{Sn}_y\text{O}$ ". 0.5 M sol-gel solution of $\text{Ni}_{0.75}\text{Ti}_{0.25-y}\text{Sn}_y\text{O}$ was prepared under ambient condition (see section 3.1.3-b). The prepared solution showed that all $\text{Ni}(\text{CH}_3\text{COO})_2 \cdot 4(\text{H}_2\text{O})$ salt was dissolved in the solution and transparent green colored was obtained. This indicates that addition of Sn prevent or delay the hydrolysis reaction of Ti-isopropoxide in the mixture.

Single layer of NiO:Ti:Sn was prepared by dipping the substrates in the prepared sol-gel solutions (see section 3.1.3-b). Then, they were annealed at 350° for 1.5-2 hours.

4.2.1: Cyclic Voltammetry (CV)

Cyclic voltammograms was measured for prepared NiO films doped with Ti and Sn (figure 4.11). The Sn was prepared with different concentrations that compensate Ti in the structure ($\text{Ni}_{0.75}\text{Ti}_{0.25-y}\text{Sn}_y\text{O}$) with y changes from 0.01 to 0.25 mol. %. NiO:Ti:Sn have been done, during 30 cycles in 0.5 M KOH electrolyte. The potential was cycled between -0.65

and 0.65 V, versus Ag/AgCl reference electrode, at a scan rate of 10 mV/s. For NiO:Ti:Sn with Sn varies from 1% to 15%, No electrochromic activity are observed in the anodic potential range - 0.6 to an average of about About 0.2 V. Anodic current density (+J), associated with the coloration of the electrochromic layer, sharply increases for anodic potential higher than about 0.45V. the anodic current density reaches its peak at an average of about 0.56 V. like what was observed for NiO:Ti, for each CV measurement, the anodic current density peaks was found to slightly shift to higher potential with increasing number of cycles. Also, all CV measurements showed current peak at 0.65 V related to oxygen evolution [98]. A single cathodic current density peak associated with the film bleaching is observed at about an average of 0.37 V. Further, the cathodic peaks are observed to be slightly shifted towards lower potential value.

The sharp increase of anodic potential, and the cathodic current peak was found to have higher values for NiO:Ti:Sn films than their NiO:Ti counter parts. This could be attributed to the morphology or structure change due to Sn dopants. As recorded by D. Park [25], existence of Zn inhibits crystallization of TiO₂ and made slight changes in the structure. Hence we expect that Sn will have same effect as Zn. The inhibition of crystallization and maintaining amorphous structure is expected to enhance the electrochromic properties as was observed for Zn dopants [25]. In addition, as observed for NiO:Ti, for a given CV measurement, the slight shift in the peaks position, for the anodic and cathodic current density,

could be attributed to the slight difference in reaction nature of the hydroxide/oxyhydroxide phases upon cycling [25, 31, 80].

The NiO:Ti:Sn, with Sn molar concentration above 5% (15 and 25%), showed an irregular CV shape and a high oxygen related anodic current (compared to coloration anodic current peak). This could be due to solubility limit of Sn within TiO₂ matrix and formation of other phases related to Sn (further future work needed to explain the results). Accordingly, we expect for this composition (25% of Sn) to have poor electrochromic properties. Hence, the results concerned the Sn contents of 15 and 25% will not be presented for other experiments.

The anodic and cathodic charge densities (Q_a and Q_c respectively) were calculated from current density versus time graph (figure 4.12).

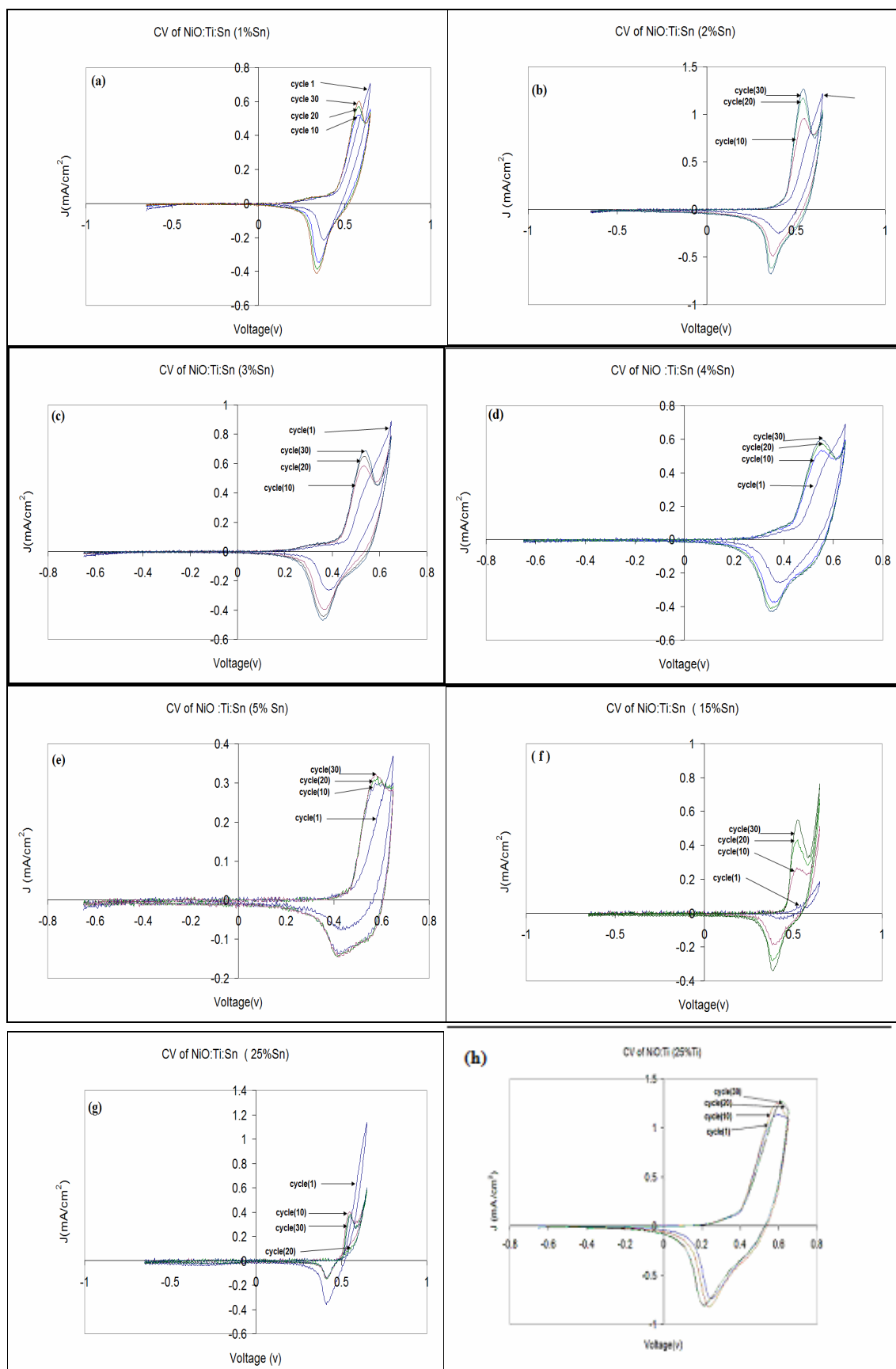


Fig. (4.11): Cyclic voltammetry measurements for cycles no 1, 10, 20, and 30 for $\text{Ni}_{0.75}\text{Ti}_{0.25-y}\text{Sn}_y$ ($\text{NiO}:\text{Ti}:\text{Sn}$) with y values a) 0.01 b) 0.02 c) 0.03 d) 0.04 e) 0.05 f) 0.15 and g) 0.25. h)0

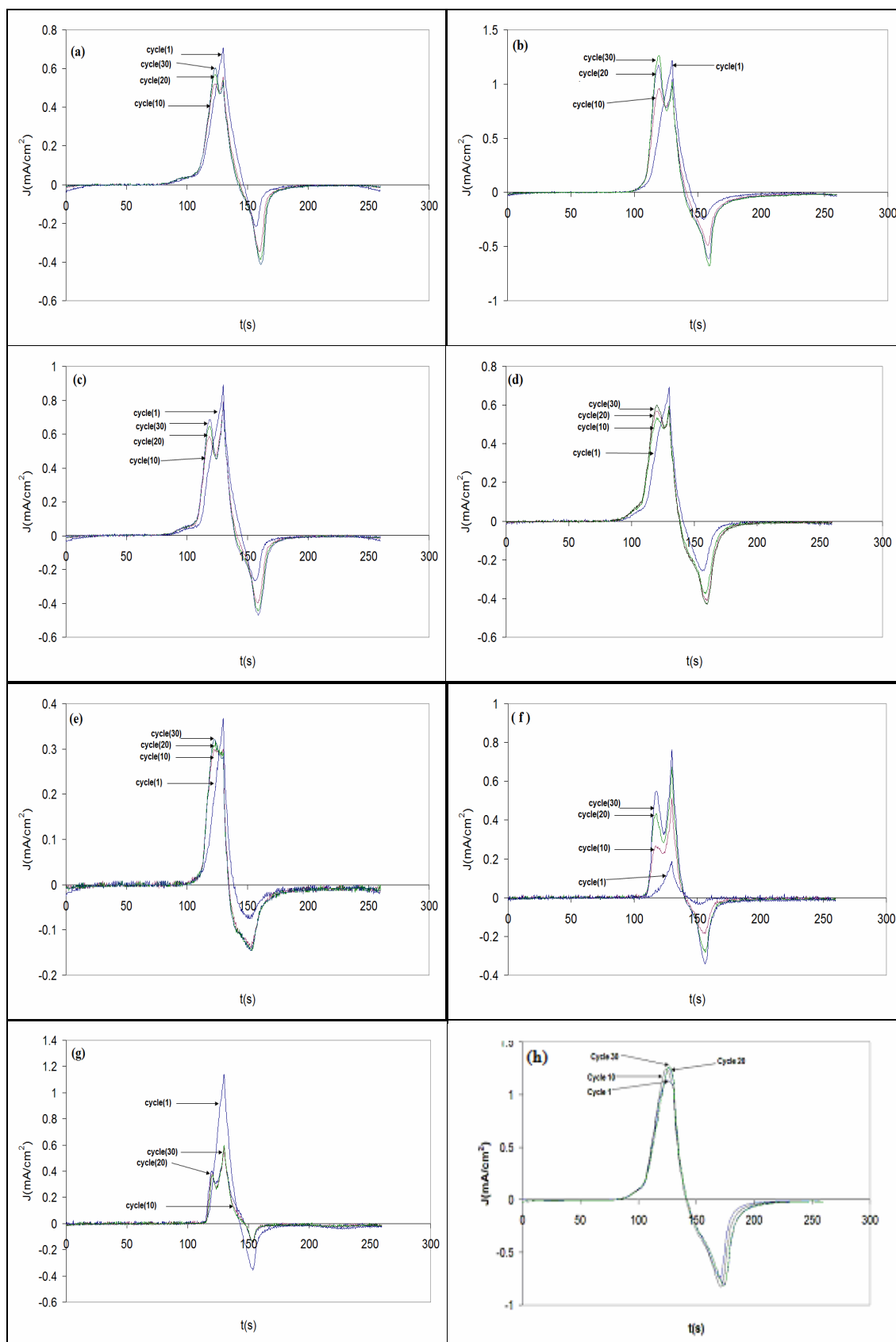


Fig. (4.12): Current density with time for cycles no 1, 10, 20, and 30 for $\text{Ni}_{0.75}\text{Ti}_{0.25-y}\text{Sn}$ ($\text{NiO}:\text{Ti}:\text{Sn}$) with y values a) 0.01 b) 0.02 c) 0.03 d) 0.04 e) 0.05 f) 0.15 and g) 0.25 h) 0

Both anodic and cathodic current densities (+J and -J) peaks are observed to increase with increasing number of cycles. This indicate an increase in the anodic and charge densities (Q_a and Q_c) asociated with coloration and bleaching of the layer. However, Q_c will be considered to be the charge density needed for coloration or bleaching of the electrochromic layer. The calculated Q_a , Q_c and Q_a/Q_c for cycled NiO:Ti films are shown in table 4.3.

Table (4.3): calculated Q_a , Q_c and Q_a/Q_c for cycles 1, 10, 20, and 30 of NiO doped with different molar concentrations of Ti and Sn

Sample composition	Cycle number	Q_a (mC)	Q_c (Mc)	Q_a/Q_c
$Ni_{0.75}Ti_{0.24}Sn_{0.01}O$	1	12.47	3.12	3.99
	10	11.17	4.94	2.26
	20	11.16	5.62	1.98
	30	11.21	6.12	1.83
$Ni_{0.75}Ti_{0.23}Sn_{0.02}O$	1	18.95	5.27	3.59
	10	19.86	9.78	2.03
	20	21.48	11.82	1.81
	30	21.72	12.89	1.68
$Ni_{0.75}Ti_{0.22}Sn_{0.03}O$	1	14.61	4.02	3.63
	10	14.23	6.23	2.28
	20	14.46	7.22	2.00
	30	14.69	7.84	1.87
$Ni_{0.75}Ti_{0.21}Sn_{0.04}O$	1	10.91	4.84	2.25
	10	11.81	7.68	1.53
	20	12.24	8.55	1.43
	30	12.49	8.99	1.38
$Ni_{0.75}Ti_{0.20}Sn_{0.05}O$	1	4.32	2.29	1.88
	10	4.78	3.95	1.21
	20	4.80	4.10	1.17
	30	4.77	4.14	1.152
$Ni_{0.75}Ti_{0.10}Sn_{0.15}O$	1	1.97	0.64	3.07
	10	6.59	3.08	2.13
	20	9.13	4.47	2.04
	30	10.78	5.29	2.03
$Ni_{0.75}Sn_{0.25}O$	1	13.44	6.04	2.22
	10	8.57	2.38	3.60
	20	7.63	2.22	3.43
	30	7.39	2.16	3.42

For given composition, after 10 cycles, Q_a showed almost a stable value with increasing cycles (except for 15 and 25 mol. %). Normally Q_a must increase with increasing cycle no up to certain cycle no. But, as quoted before, evolution of oxygen masks the real value of Q_a . In fact, the slight shift of anodic current peak towards higher potential is associated with a decreases the oxygen evolution current. This is why we may observe almost stable value for Q_a compare with that undoped.

As expected, the value of Q_c always increases with increasing cycles. The increase in the current density with cycles indicates that the amount of coloring sites available for the redox reaction increases and is still unsaturated [32].

The ration Q_a/Q_c is found to be higher than one and decreases with number of cycles. We believe that for much higher number of CV cycles, the value of Q_a/Q_c decrease more until it become stable, when reaching coloration sites saturation, at a value close one (further work needed for verification). Q_a/Q_c is expected to decrease due to the decrease of oxygen related current, which is associated with the shift of anodic current towards higher potential with increasing cycles.

4.2.2 Optical properties

a) Transparency

For reference transparencies, the transmission of the glass and FTO/glass substrate was scanned versus air, in the visible range, at a

wavelength varied from 290-800 nm. Transmission spectra, at same wavelength range, for films of different deposited layers on glass substrates and on FTO/glass substrates was also performed. Moreover, the transmission of spectra for films during CV measurements (coloring and bleaching), was carried out at a wavelength of 550 nm for the cycle number 29 and 30. Like those for NiO:Ti, The measurements were carried out, for the NiO:Ti:Sn electrodes, in the three electrode electrochemical cell, at normal incident angle against a reference cell that contains 0.5 M KOH; transmittance was always reset to 100 % before running each CV experiment.

As quoted before, Color change in the visible light is one important feature of electrochromic devices; the more transmittance in the bleach state (T_b) and less transmittance in color state (T_c) is a need for efficient electrochromic device. Thickness of the film is known to affect the transparency of the thin film [40]. For this, transparency of the film was scanned in, the visible range, for different thickness films (figure 4.13). Multiple layer films, and hence different thickness films, were obtained by making multiple insertion of substrate in the sol-gel solution (see section 3.1.3 for procedure).

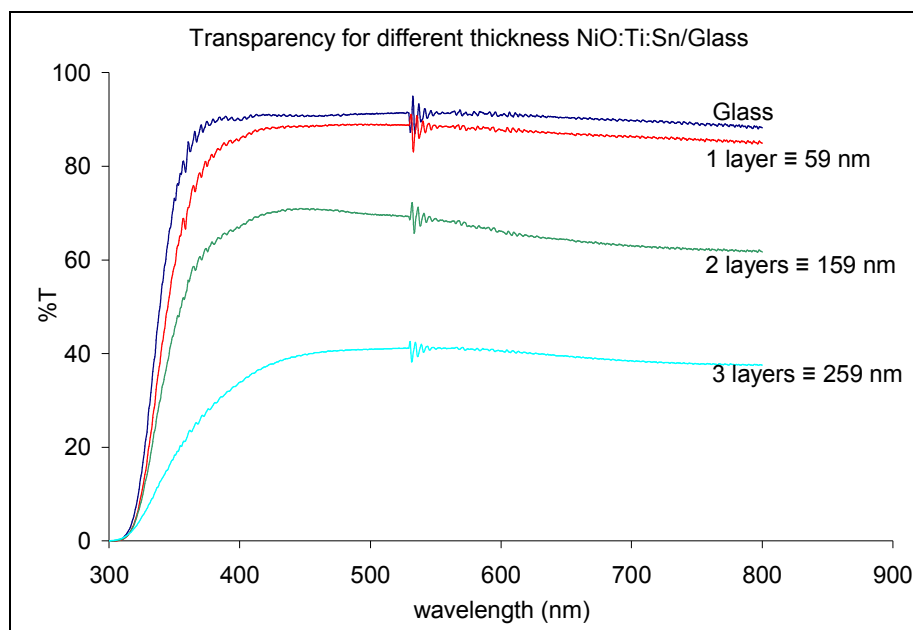


Fig. (4.13): Transparency for different layer NiO:Ti:Sn films.

The reference transparency of glass reached a value of 91 % relative to air. One layer film showed a high transparency of about 88 % (97 % of glass transparency). Other films of two layers and three layers, showed a transparency, with respect to air, of an average 65 % and 39 % respectively. Hence, as film thickness decrease, the film transparency in the bleach state will be better. Due to this, Unlike the NiO:Ti films in which we used double layer, single layer films was chosen to perform experiments for NiO:Ti:Sn.

To observe the effect of the FTO/Glass substrate, transparency was scanned versus air for FTO/glass and for different thickness films. The obtained scanning results are shown in figure 4.13. As expected, the transparency of the film was observed to decrease due to FTO layer. The transparency of FTO reached an average of about 80 % with respect to air.

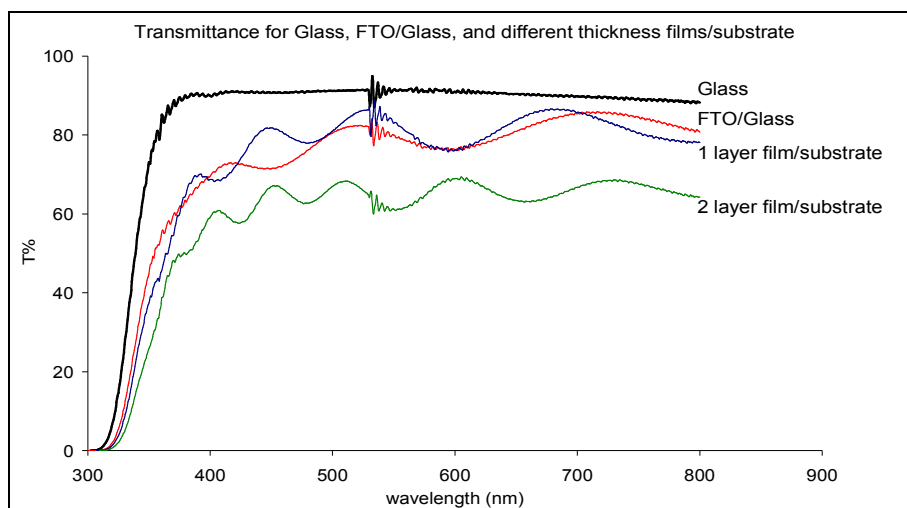


Fig. (4.14): Visible range Transparency (T) spectra for Glass, FTO/glass substrate, and different thickness films/substrate; air is set as a reference.

Relative to air, the transparency of our electrochromic films decreased to an average of about 78 % for single layer film and 61 % for double layer film. However, the transparency, for single layer film, still have high value and reached about 83% at a wavelength of 550 nm.

Figure 4.14 shows the transparency at a wavelength of 550 nm, during CV measurements (cycles 29 and 30), for NiO:Ti:Sn electrochromic films with different Sn molar concentrations.

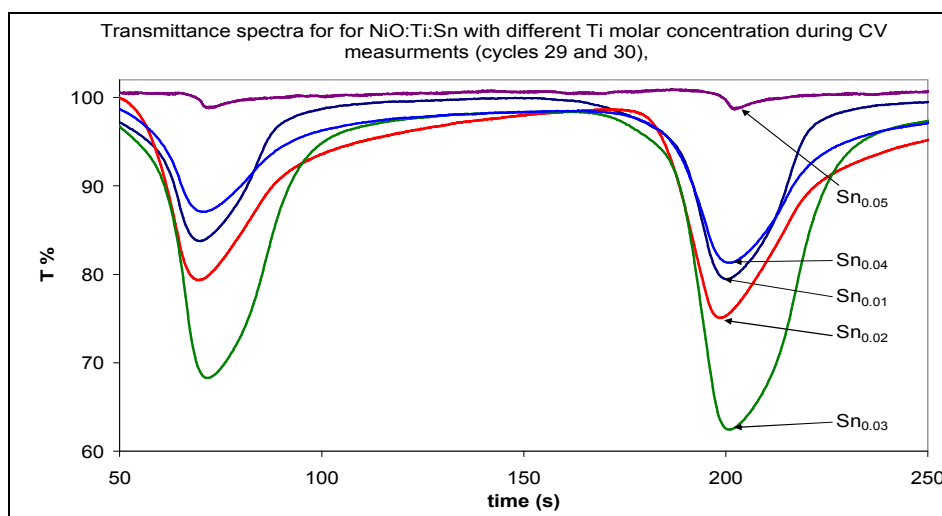


Fig. (4.15): Coloration and bleaching transparency (T) spectra, during CV measurements (cycles 29 and 30), for double layer NiO:Ti:Sn with different Sn molar concentrations.

As observed for NiO:Ti, All films of NiO:Ti:Sn showed a high transparency during bleaching process. However, the transparency in the bleaching process (T_b) slightly decreases with cycling. This is as mentioned above, due to wetting of the layer and freshly precipitated Ni(OH)₂ [98, 25, 31, 32, 80]. It was also observed that Transparency in the color state, T_c , decreases with Sn contents until reaching its minimum (~ 62 %) at Sn contents of 3 % mol. (12 % of Ti concentration). T_c increases again until reaching its minimum for Sn contents of 5 mol. %. This could be due to solubility limit of Sn within Ti matrix embedded into NiO (further future work on structure is needed to confirm this). Also, T_c is observed to decrease with increasing cycle number. This is due to not reaching the saturation, for the film coloration sites available, in the electrochemical reaction [32].

From Figure 4.15 that represents transparency and current density during CV measurement (cycle 30), we can observe that the coloration of the film is associated with the anodic current density (+J). While the bleaching process is associated with the cathodic current density (-J).

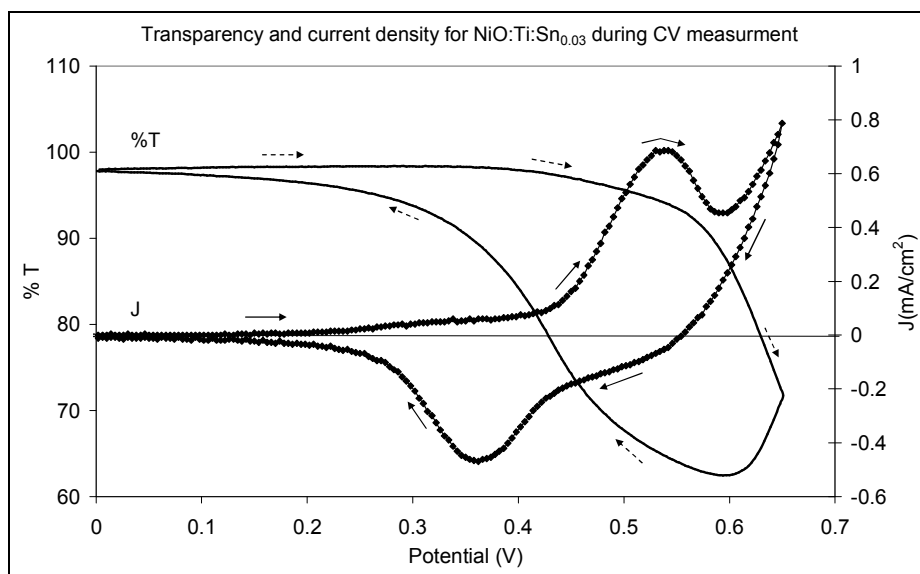


Fig. (4.16): Transparency and current evolution during CV measurement for NiO:Ti:Sn0.03 layer. (→) indicates the current evolution and (- - - →) indicates corresponding Transparency evolution.

Since the cathodic current is the current for a complete change between coloration and transparency, we can use it to calculate the charge (Q_c) needed to color the layer. The anodic current is not used in calculation due to the oxygen evolution during coloration of the layer.

For the different NiO:Ti:Sn films, the calculated contrast ratio (T_b/T_c) and coloration efficiency (CE), for cycle 30, are tabulated in table 4.4.

Table (4.4): calculated contrast ratio (T_b/T_c) and coloration efficiency (CE) for cycle 30 of NiO:Ti films doped with different molar concentration of Sn. NiO:Ti0.25 is presented here for comparison.

Sample composition	Q_c (mC/cm ²) for cycle 30	T_b	T_c	T_b/T_c	CE(cm ² /C)
Ni _{0.75} Ti _{0.25} O	22.63	98.81	53.83	1.84	11.7
Ni _{0.75} Ti _{0.24} Sn _{0.01} O	6.12	99.70	79.45	1.25	16.1
Ni _{0.75} Ti _{0.23} Sn _{0.02} O	12.90	96.17	75.00	1.28	8.4
Ni _{0.75} Ti _{0.22} Sn _{0.03} O	7.84	98.00	62.40	1.57	25.0
Ni _{0.75} Ti _{0.21} Sn _{0.04} O	9.00	97.70	81.30	1.20	8.9
Ni _{0.75} Ti _{0.20} Sn _{0.05} O	4.14	100.00	98.60	1.02	2.2

For different Sn contents, T_b/T_c was observed to increase with Sn contents until reaching its maximum (1.57) at Sn contents of 3 mol. %. For higher Sn contents, T_b/T_c decreases with Sn contents and reaches its minimum for the highest content of Sn (5 mol. %). Associated with highest contrast ratio, the film with 3 mol. % of Sn was also found to have the highest CE (25 %). 3 mol. % of Sn could be the highest contents (solubility limit) that can substitute Ti within the TiO_2 matrix, without introducing new phases corresponds to Sn. This could explain the best results for this composition. It was found by D. Park that no XRD peaks corresponds to Zn phases exist when 10 mol. % of Zn substitutes Ti in TiO_2 [25]. However, XRD peaks for ZnO was observed when substituting Ti by 15 mol. %. This is an indication that solubility limit of Zn into TiO_2 matrix lies between 10 and 15 mol. %. Indeed, introduced ZnO phase was found to negatively affect the electrochromic properties of the film.

$NiO:Ti:Sn_{0.03}$ showed a higher CE (more than two times) than $NiO:Ti_{0.25}$. Sn dopant represents a material that is the same as the substrate material (SnO_2 doped with F). Hence better adhesion to the substrate was expected when doping with Sn. This would in turn enhance the electrochromic properties of the films.

b) Film thickness

For FTO/glass substrate and $NiO:Ti:Sn$ films/substrate, T_{max} and T_{min} were drawn on interference fringes (figure 4.16) in order to determine the thickness of the films.

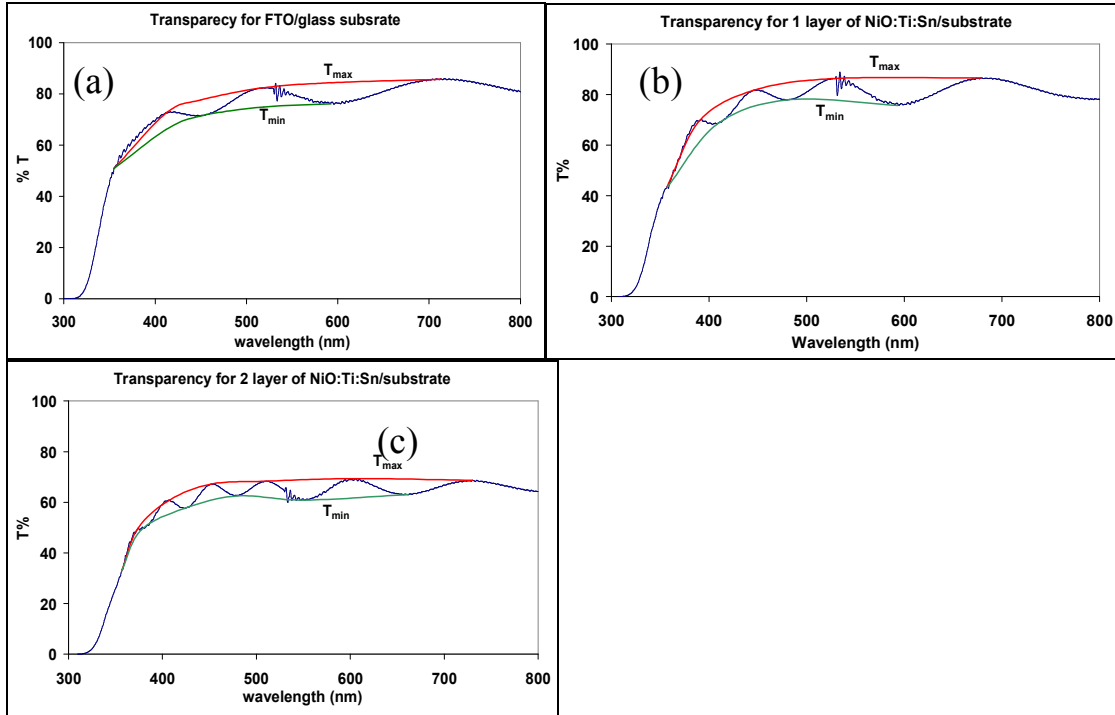


Fig. (4.17): Transmission spectra with T_{max} and T_{min} for (a) FTO/glass substrate, (b) 1 layer film/substrate, and (c) 2 layer film/substrate.

Note that we have two types of films (FTO and NiO:Ti:Sn) are deposited on glass substrate. Despite this, the above method for calculating film thickness is still valid. This is because the refractive index of the electrochromic film (NiO based film) is very similar to FTO thin film (SnO₂ based film) [104-105]. Hence, for thin film calculation, we can consider both films as a single film on glass substrate. Therefore, finding the thickness of the two films/glass and subtract FTO film thickness will give you the electrochromic film thickness alone.

The average transmittance of the glass in the visible range was found to have an average of 91%. Hence, the calculated glass refractive index (n_1) from equation (2.6) is 1.55. Taking n_0 equals 1 for air and calculating n_2 for film from equation (2.8), we can calculate the films thickness on glass from (2.9) and (2.7). The calculated films thicknesses are presented in table 4.5.

Table (4.5): calculated film thickness for different deposited films on FTO/Glass

Sample	Average thickness (nm)
FTO	557
1 layer NiO:Ti:Sn/FTO	616
2 layer NiO:Ti:Sn/FTO	716
1 layer NiO:Ti:Sn	59
2 layer NiO:Ti:Sn	159
3 layers NiO:Ti:Sn	259

FTO thickness increases by 59 nm for single dipping in the sole-gel. However, the film increased by other 100 nm when dipped for second time. This is in fact expected because first layer was deposited on FTO which is not same material. But the second layer was deposited on the first layer of same material. Hence one can expect to have higher thickness when depositing on same material due to better adhesion interface. The third layer thickness was estimated depending on second layer thickness.

c) *Band-gap determination*

In energy band-gap (or optical band-gap) determination, the strong absorption region (Fig.2.9) must obviously be considered. In its bleach state (as prepared), NiO based electrochromic films appears to be transparent. Hence, they are expected to have large energy band-gaps, in the range 3 to 4 eV, which correspond to photon wavelength range of about 300–400 nm (near-ultraviolet region). While they are absorbed, these photons induce electronic transitions from the valence band to the empty energy states in the conduction band. In this region, one can estimate the value of the optical band-gap using the relation [106-107]:

$$\alpha h\nu \propto (h\nu - E_g)^\eta \quad (4.1)$$

where α is the absorption coefficient, $h\nu$ is the photon energy, E_g is the band-gap at the same wave number, and η is a constant taking the values 1/2 and 2, depending on whether the optical transitions are respectively direct allowed or indirect allowed. For the direct allowed transition, extrapolated to zero, of the linear part for the curve $(\alpha h\nu)^2$ versus $h\nu$, gives the value of E_g . For the indirect allowed transitions, the curve which has to be drawn and extrapolated to zero, in order to determine the E_g , is $(\alpha h\nu)^{1/2}$ versus $h\nu$ [106-107].

In the strong absorption region, one can define the transmission T by the following relation [108]

$$T \propto \exp(-\alpha d) \quad (4.2)$$

Thus using the data from the transmission spectra T of the film and knowing the thickness d value, absorption coefficient (α) can be directly calculated.

For different thickness films on glass and on FTO/glass substrate, transparency spectra (Fig. 4.12 and Fig. 4.13) were used to calculate absorption coefficient (α) at different wavelength. $(\alpha h\nu)^2$ versus $h\nu$ was drawn (figure 4.17), assuming direct optical allowed transition [109], in order to determine the optical band-gap E_g for as prepared films.

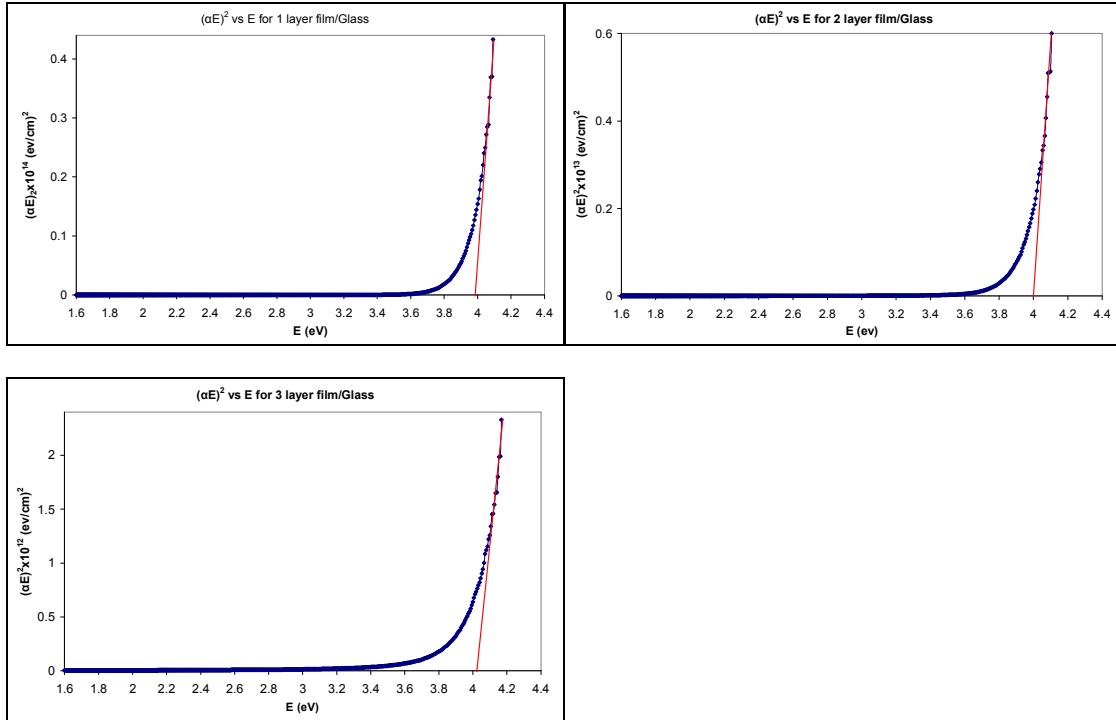


Fig. (4.18): Plot of $(\alpha E)^2$ versus photon energy E for different thickness NiO:Ti:Sn films deposited on glass substrate.

For all films, the energy band-gap, E_g , was observed to have a value around 4 eV. This reflects the transparent property of the prepared films in the bleach state. The observed slight increase of E_g is due to the slight increase of carrier concentration with increasing film thickness. This variation can be explained by the Burstein-Moss effect [25,110]. It shows that for the transparent thin film E_g increases with the carrier concentration.

4.2.3. Conclusion

Doping NiO:Ti with Sn was found to enhance the electrochromic properties of the prepared electrochromic films. Compared to NiO:Ti, a remarkable delays the Titanium isoproboxide hydrolysis that negatively affects the quality of electrochromic properties. This will allow an easy

deposition of the Sn-doped films under ambient atmosphere. Same result was noticed when doping NiO:Ti by Zn [25]. Also doping with Sn is expected to inhibit crystallization as it was observed for Zn [25] (more future work is needed). Less grain size allowed higher surface area to be exposed to electrochemical reaction. Hence higher coloration and consequently higher coloration efficiency will be obtained. Moreover, doping with Sn enhances the adhesion of the film to the substrate because it is from same material. Hence better link will occur at the interface between film and substrate. This in turn will positively affect the electrochromic properties.

Suggestions for Further Work

We suggest the following for our new electrochromic electrode NiO:Ti:Sn for future work:

- 1) Doing the work for higher no cycles (couple of thousands).
- 2) Doing more analysis for the films such as: XRD, PL, SEM, TEM, AFM, etc.
- 3) Preparing NiO thin films using different techniques such: Electrochemical Deposition (ECD), Chemical Bath Deposition (CBD).
- 4) Studing electrochromic properties when the films aneling with different tempretures.
- 5) Studing effect of thickness on electrochromic properties.
- 6) Studing the characteristics of the previous films with different electrolytes & different electrolyte concentrations.
- 7) Doping with different materials such as: F, Li ,etc .

References

- [1] Ferreira F F, TabacniksM H, Fantini M C A, Faria I C and Gorenstein, *Electrochromic nickel oxide thin films deposited under different sputtering conditions*, **A Solid State Ionics**, **86–88** (1996) 971-976.
- [2] Scarminio J, Urbano A, Gardes B J and Gorenstein, *Invistigation of anode materials for lithium-ion batteries*, **J. Mater. Sci. Lett**, **562** (1992) 11.
- [3] Fantini M C A, BenerraG H, Carvalho C R C and Gorenstein A 1996 *Proc. SPIE, Electrochromic properties and temperature dependence of chemically deposited Ni(OH)_x thin films*, Online Publication Date: Feb 23, 2005, <http://dx.doi.org/10.1117/12.49215>, **1536** (1996) 81.
- [4] I. Hotovy, J. Huran, P. Siciliano, S. Capone, L. Spiess, V. Rehacek, *Sol-gel prepared NiO thin films for electrochromic applications*, **Sensor Actuator**, **B78** (2001) 126–132.
- [5] A. F. Wells, *Structural Inorganic Chemistry*, **5th Ed**, Clarendon press, Oxford, (1984) p 538.
- [6] E. Antolini, *Sintering of Li_xNi_{1-x}O solid solutions at 1200°C*, **J. Mater. Sci**, **27** (1992) 3335–3340.
- [7] J. S. E. M. Svensson, C. G. Granqvist, *Electrochromic hydrated nickel oxide coatings for energy efficient windows: Optical properties and coloration mechanism*, **Appl. Phys. Lett**, **49** (1986) 1566–1568.

- [8] P. C. Yu, G. Nazri, C. M. Lampert, *Proc. SPIE, Spectroscopic and electrochemical studies of electrochromic hydrated nickel oxide films*, 3rd international conference on optics and electrooptics, Innsbruck, Austria, April 14-18, **653** (1986) 16–24.
- [9] J. Nagai, *Characterization of evaporated nickel oxide and its application to electrochromic glazing*, *Sol Energ Mat Sol C*, **31**(2) (1993) 291-299.
- [10] I. Bouessay, A. Rougier, J.-M. Tarascon, *Electrochemically inactive nickel oxide as electrochromic material*, *J. Electrochem. Soc.*, **151** (2004) H145–H152.
- [11] E. Avendano, L. Berggren, G. A. Niklasson, C. G. Granqvist, A. Azens, *Electrochromic materials and devices: Brief survey and new data on optical absorption in tungsten oxide and nickel oxide films*, *Thin Solid Films*, **496** (1) (2006) 30–36.
- [12] G. Boschloo, A. Hagfeldt, *Spectro electro chemistry of nanostructured NiO*, *J. Phys. Chem. B*, **105** (2001) 3039–3044.
- [13] E. L. Miller, R. E. Rocheleau, *Electrochemical and electrochromic behavior of reactively sputtered nickel oxide*, *J. Electrochem. Soc.*, **144** (1997) 1995–2003.
- [14] X. Chen, X. Hu, J. Feng, *Nanostructured nickel oxide films and their electrochromic properties*, *Nanostruct. Mater.*, **6** (1995) 309–312.

- [15] Z. Xuping, C. Guoping, *The microstructure and electrochromic properties of nickel oxide films deposited with different substrate temperature*, **Thin Solid Films**, **298** (1997) 53–56.
- [16] W. Estrada, A. M. Andersson, C. G. Granqvist, *Electrochromic nickel oxide-based coatings made by reactive dc magnetron sputtering preparation and optical properties*, **J. Appl. Phys**, **64** (1988) 3678–3683.
- [17] I. Bouessay, A. Rougier, P. Poizot, J. Moscovici, A. Michalowicz and J.-M. Tarascon, *Electrochromic degradation in nickel oxide thin film : a self-discharge and dissolution phenomenon*, **Electrochim. Acta** **50**(18) (2005) 3737-3745.
- [18] A. Azens, C. G. Granqvist, *Electrochromic smart windows: energy efficiency and device aspects*, **J. Solid State Electrochem**, **7** (2003) 64–68.
- [19] P. K. Shen, H. T. Huang, A. C. C. Tseung, *Study of electrodeposited tungsten trioxide thin films*, **J. Mater. Chem**, **2** (1992) 1141–1447.
- [20] A. Surca, B. Orel, B. Pihlar, P. Bukovec, *Optical, spectro electrochemical and structural properties of sol-gel derived nickel oxide electrochromic film*, **J. Electroanal Chem**, **408** (1996) 83.
- [21] P.K. Sharma, M.C.A. Fantini, A. Gorenstein, *Synthesis, characterization and electrochromic properties of NiOxHy thin film*

- prepared by a sol-gel method, Solid State Ionic*, **113-115** (1998) 457-463.
- [22] A. Azens, C.G. Granqvist, *Electrochromism of sputter deposited Ni-Cr oxide films*, *Appl Phy*, **84** (1998) 6454.
- [23] N. Penin, A. Rougier, L. Laffont, P. Poizot and J.-M. Tarascon, *Improved cyclability by tungsten addition in electrochromic NiO thin films*, *Sol Energ Mat Sol C*, **90** (2006) 422.
- [24] X. Lou, X. Zhao, J. Feng, X. Zhou, *Electrochromic properties of Al doped B-substituted NiO films prepared by sol-gel* *Prog. Org Coat*, **64** (2-3) (2009) 300-303.
- [25] Dae Hoon Park, *Optimization of nickel oxide- based electrochromic thin films*, Ph. D. Thesis, Bordeaux I University, France,(2006).
- [26] A. Agrawal, H. R. Habibi, R. K. Agrawal, J. P. Cronin, D. M. Roberts, R. S. Caron-Popowich, C. M. Lampert, *Effect of deposition pressure on the microstructure and electrochromic properties of electron-beam-evaporated nickel oxide films*, *Thin Solid Films*, **221**(1-2) (1992) 239–253
- [27] M. Utriainen, M. Kröger-Laukkanen, L. Niinistö, *Mater, Studies of NiO thin film formation by atomic layer epitaxy*, *Mater. Sci. Eng : B* **54** (1-2) (1998) 98–103.

- [28] P. S. Patil, L.D. Kadam, *Preparation and characterization of spray pyrolyzed nickel oxide (NiO) thin films*, **Appl. Surf. Sci.**, **199** (2002) 211–221.
- [29] M. Chigane, M. Ishikawa, *Enhanced Electrochromic Property of Nickel Hydroxide Thin Films Prepared by Anodic Deposition*, **J. Electrochem. Soc.**, **141** (1994) 3439–3443.
- [30] R. Cerc Korošec, P. Bukovec, *Sol-gel processing for conventional and alternative energy*, **Thermochim. Acta**, **410** (2004) 65–71.
- [31] A. Al-Kahlout, *Electrochromic properties and coloration mechanisms of sol-gel NiO-TiO₂ layers and devices built with them*, Ph. D. Thesis, University of Saarland and Leibniz- Institut für Neue Materialien- (INM) and University of Saarland,(2006).
- [32] A. Al-Kahlout, S. Heusing, M.A. Aegerter, *Electrochromism of NiO-TiO₂ sol- gel layer*, **J. Sol-Gel Sci. Technol.** **39** (2006) 195.
- [33] P. M. S. Monk, S. P. Akhtar, J. Boutevin and J. R. Duffield, *Toward the tailoring of electrochromic bands of metal – oxide mixtures*, **Electrochim. Acta** **46** (2001) 2091.
- [34] P. M. S. Monk, R. J. Mortimer and D.R. Rosseinsky, *Electrochromism: Fundamentals and Applications*, Weinheim, VCH, 1995.

- [35] I. Hamberg and C. G. Granqvist, *Evaporated Sn-doped In_2O_3 films :basic optical properties and applications to energy –efficient windows*, **J. Appl. Phys.** **60** (1986) R123.
- [36] C. G. Granqvist and A. Hultåker, *Transparent and conducting ITO films :new developments and applications*, **Thin Solid Films.** **411** (2002) 1.
- [37] C. G. Granqvist, *Handbook of Inorganic Electrochromic Materials*, Elsevier, Amsterdam, 1995, Reprinted 2002.
- [38] C.G Granqvist, *Transparent conductors as solar energy materials: A panoramic review* , **Sol Energ Mat Sol C.** **91** (2007) 1529-1598.
- [39] G. J. Exarkhos and X.-D. Zhou, *Discovery-based design of transparent conducting oxide films*, **Thin Solid Films** **515** (2007) 7025-7052.
- [40] I. Saadeddin, *Preperation and characterization of new transparent conducting oxides based on SnO_2 and In_2O_3 :ceramics and thin films*, *PhD. thesis*, Bordeaux I University, Bordeaux, France, 2007.
- [41] D. Mergel, M. Schenkel, M. Ghebre and M. Sulkowski, *Structural and electrical properties of In_2O_3 :Sn films prepared by radio-frequency sputtering*, **Thin Solid Films.** **392** (2001) 91-97.
- [42] P. M. S. Monk, R. J. Mortimer and D. R. Rosseinsky, *Electrochromism and Electrochromic Devices*, Cambridge University Press (2007) 421.

- [43] R. J. Mortimer, *Organic electrochromic materials*, *Electrochimica Acta*, **44**(18) (1999) 2971-2981.
- [44] A. Samat and R. Guglielmetti, Kirk-Othmer, *Encyclopedia of Chemical Technology (5th Edition)*, John Wiley & Sons, 6 (2004) 571.
- [45] J. N. Yao, P. Chen, A. Fujishima, *Electrochromic behavior of electrodeposited tungsten oxide thin films*, *J. Electroanal. chem.* **406** (1-2) (1996) 223-226.
- [46] Vondrák J., Sedlaríková M., Hodal T, *Polymer Gel Electrolytes for Electrochromic Devices*, *Electrochimica Acta* **44** (1999) 3067
- [47] J. N. Yao, K. Kashimoto, A. Fujishima, *Photochromism induced in an electrolytically pretreated MoO₃ thin film by visible light*, *Nature* **355** (1992) 624-626.
- [48] M. R. Tubbs, *MoO₃ layers — optical properties, colour centres, and holographic recording*, *Phys. Status Solidi A* **21** (1)(1974) 253-260.
- [49] C. Bechinger, S. Ferrere, A. Zaban, J. Sprague, B. A. Gregg, *Photoelectrochromic windows and displays*, *Nature* **383** (6601) (1996) 608-610.
- [50] R. D. Rauh, *Electrochromic Windows-An Overview*, *Electrochim. Acta*, **44** (1999) 3165.

- [51] K. Bange, *Colouration of tungsten oxide films: A model for optically active coatings*, **Sol. Energy. Mater.Sol. Cells** **58**(1) (1999) 1-131.
- [52] A. Azens, G. Gustavsson, R. Karmhag and C. G. Granqvist, *Electrochromic devices on polyester foil*, **Solid State Ionics**, **165** (1-4) (2003) 1-5.
- [53] J. N. Huiberts, R. Griessen, J. H. Rector, R. J. Wijngaarden, J. P. Dekker, D. G. de Groot and N. J. Koeman, *Yttrium and Lanthanum hydride films with switchable optical properties*, **Nature**, **380** (1996) 231.
- [54] R. J. Mortimer and D. R. Rosseinsky, *Iron hexacyanoferrate films : spectroelectrochemical distinction and electrodeposition sequence of 'soluble' (K⁺-containing) and 'insoluble' (K⁺-free) Prussian Blue, and composition changes in polyelectrochromic switching*, **J. Chem. Soc., Dalton Trans.**, **9** (1984) 2059-2062
- [55] F. Decker, S. Passerini, R. Pileggi and B. Scrosati, *The electrochromic process in non-stoichiometric nickel oxide thin film electrodes*, **Electrochim. Acta** **37**, (1992) 1033-1038.
- [56] I. Bouessay, A. Rougier, B. Beaudoin and J.-B. Leriche, *pulsed laser-deposited nickel oxide thin films as electrochromic anodic materials*, **Appl. Surf. Sci.** **186** (2002) 490.
- [57] A. Fukazawa and M. Chihiro, *Electrochromic element*, **European patent EP 1434083 (A2)**, 2004.

- [58] D. Calloway, *Beer – Lambert law*, **J. Chem. Educ.** **74**(7) (1997) 744.
- [59] <http://www.sage-ec.com> (Date accessed: 10 Feb 2012).
- [60] J.S.E.M. Svensson and C.G. Granqvist, *Electrochromic coatings for “smart windows”*, **Sol Energ Mater.** **12** (1985) 391.
- [61] <http://fr.wikipedia.org/wiki/Nickel> (Date accessed: 12 Feb 2012).
- [62] N. N. Greenwood and A. Earnshaw, *Chemistry of the Elements*, Oxford: Pergamon, (1984) p1336.
- [63] Y. Ushio, A. Ishikawa and T. Niwa, *Degradation of the electrochromic nickel oxide film upon redox cycling*, **Thin Solid Films** **280** (1996) 233.
- [64] A.-L. Larsson and G.A. Niklasson, *Infra emittance modulation of all-thin-film electrochromic devices*, **Mater. Lett.** **58** (2004) 2517–2520.
- [65] K.-S. Lee, H.-J. Koo, K.-H. Ham, W.-S. Ahn, *Bull. Kor, Electronic Structure of Oxygen in the Defective Nickel Monoxide* **Chem. Soc.**, **16** (2) (1995) 164.
- [66] R. Merlin, *Electronic Structure of NiO*, **Phys. Rev. Lett.** **54** (1985) 2727.
- [67] K. Lascelles, L. G. Morgan, D. Nicholls and D. Beyersmann, *“Nickel Compounds” in Ullmann's Encyclopedia of Industrial Chemistry*, Wiley-VCH, Weinheim, 2005.

- [68] U.S. Dept. of Health and Human Services, *Toxicology and Carcinogenesis Studies of Nickel Oxide*, 7(1996) 451.
- [69] P. Oliva, J. Leonardi, J. F. Laurent, C. Delmas, J. J. Braconnier, M. Figlarz, F. Fievet and A. de Guibert, *Review of the structure and the electrochemistry of nickel hydroxides and oxy-hydroxides*, *J. Power Sources*, 8 (1982) 229.
- [70] S. Le Bihan, J. Guenot and M. Figlarz, *Sur la cristallogénèse de l'hydroxyde de nickel Ni(OH)₂*, *C.R. Acad. Sci., Ser. C* 270 (1970) 2131.
- [71] M. I. Carpenter and D. A. Corrigan, *Photoelectrochemistry of nickel – hydroxide thin-films*, *J. Electrochem. Soc.* 136(4) (1989) 1022-1026.
- [72] R. Barnard, C. F. Randell and F. L. Tye, *Studies concerning charged nickel hydroxide electrodes Part III. Reversible potentials at low states of charge*, *J. Electroanal. Chem.* 119 (1981) 17-24.
- [73] O. Glemser, J. Einerhand, *Über höhere Nickelhydroxyde*, 2. *Anorg. Allg. Chem.*, 261(1-2) (1950) 26-42
- [74] H. Bode, K. Dehmelt and J. Witte, *Zur Kenntnis der nickelhydroxidelektrode—I. Über das nickel (II)-hydroxidhydrat*, *Electrochim. Acta* 11(8) (1966) 1079-1087

- [75] G. W. D. Briggs, E. Jones and W. F. K. Wynne-Jones, *The nickel oxide electrode. Part 1*, **Trans. Faraday Soc.** **51** (394) (1955) 1433-1442.
- [76] G. W. D. Briggs, E. Jones and W. F. K. Wynne-Jones, *The nickel oxide electrode. Part 2*, **Trans. Faraday Soc.** **52** (405) (1956) 1260-1272.
- [77] F. P. Kober, *Analysis of the Charge-Discharge Characteristics of Nickel-Oxide Electrodes by Infrared Spectroscopy*, **J. Electrochem. Soc.** **112** (11) (1965) 1064-1067.
- [78] R. Barnard, G. T. Crickmore, J. A. Lee and F. L. Tye, *The cause of residual capacity in nickel oxyhydroxide electrodes*, **J. Appl. Electrochem.** **10** (1980) 61-70.
- [79] S.R Jiang, P.X Yan, B.X Feng, X.M Cai, J Wang , *The response of a NiO_x thin film to a step potential and its electrochromic mechanism*, **Mater. Chem. Phys.** **77** (2) (2003) 384-389.
- [80] M. Fantini and A. Gorenstein, *Electrochromic nickel hydroxide films on transparent/conducting substrates*, **Sol Energ Mat Sol C**, **16** (6) (1987) 487 -500.
- [81] W. Jacob, A. Keudell, T. S. Selinger, *Braz*, *Infrared analysis of thin films: amorphous, hydrogenated carbon on silicon*, **J. Phys**, **30** (2000) 508-516.
- [82] R. Swanepoel, *Determination of the thickness and optical constants of amorphous silicon*, **J. phys. E: Sci. Instrum.** **16** (1983) 1214.

- [83] J. C. Manifacier, J. Gasiot, J. Fillard, *A simple method for the determination of the optical constants n , k and the thickness of a weakly absorbing thin film*, **J. Phys. E: Sci. Instrum**, **9** (1976) 1002.
- [84] J.S.E.M. Svensson, C.G. Granqvist, *Electrochromic hydrated nickel oxide coatings for energy efficient windows: Optical properties and coloration mechanism*, **Appl Phys Lett**, **49** (1986) 1566-1568.
- [85] L. Ottaviano, A. Pennis, F. Simone, *Electrochromic nickel oxide films made by reactive r.f. sputtering from different targets*, **Surface and Interface Analysis**, **36** (2004) 1335.
- [86] K. Yoshimura, T. Miki, S. Tanemura, *Direct observation of the structure of nickel oxide electrochromic thin films by HRTEM*, **Optical Materials Technology for Energy Efficiency and Solar Energy Conversion**, Thursday 13 July 1995, San Diego, CA, USA, SPIE Proceedings, 2531 (1995) 127
- [87] T. Seike, J. Nagai, *Electrochromism of 3d transition metal oxides*,
- [88] D. B. Chrisey and G. K. Hubler, *Pulsed laser deposition of thin films*, John Wiley and Sons, New York (1994).
- [89] http://en.wikipedia.org/wiki/Pulsed_laser_deposition (Date accessed: 13 April 2010).
- [90] G. Sasikala, R. Dhanasekaran, C. Subramanian, *Electrodeposition & Optical Characterization of Cds thin films on ITO/coated glass*, **thin solid film**, **302** (1997), 71-76.

- [91] H.S.Hilal, R.M.A.Ismail, A.El-Hamouz, A.Zyoud, I.Saadeddin, *Effect of cooling rate of pre-annealed Cds thin film electrodes prepared by chemical bath deposition in enhancement of photo-electrochemical characteristics*, *electrochim Acta*, **54** (2009) 3433-3440.
- [92] <http://en.wikipedia.org/wiki/Dip-coating> (Date accessed: 13 April 2010).
- [93] M.N. Rahaman, *Ceramic Processing. Boca Raton: CRC Press, ISBN 0-8493-7285-2*, Taylor & Francis (2007) 242 - 244.
- [94] L. D. Landau and B. G. Levich, *Entrainment of fluid by the driven plate*, *Acta Phys chem*, **17** (1942) 42
- [95] L. L. Hench and J. K. West, *The sol-gel process*, *Chem. Rev.* **90**(1) (1990) 33-72.
- [96] Yoshinari Makimura, Aline Rougier, Jean-Marie Tarascon, *Cobalt and tantalum additions for enhanced electrochromic performances of nickel-based oxide thin films grown by pulsed laser deposition*, *Appl Surf Sci*, **252** (13-30) (2006) 4593-4598.
- [97] X. Lou, X. Zhao, J. Feng, X. Zhou, *Electrochromic properties of Al doped B-substituted NiO films prepared by sol-gel*, *Prog.Org.Coat*, **64** (2-3) (2009) 300-303.
- [98] Rougier, A., Rauh, D. and Nazri, *Electrochromic Materials and Applications*, G. A. (eds.), 2003–17, Pennington, NJ, Electrochemical Society proceeding, p 113, 2003

- [99] I. Serebrennikova and V.I. Birss, *Electrochemical Behavior of Sol-Gel Produced Ni and Ni-Co Oxide Films*, **J. Electrochem. Soc.**, **144**(2) (1997) 566-571.
- [100] http://en.wikipedia.org/wiki/Color_vision#cite_note-1
- [101] Yude Wang, Chunlai Ma, Xiaodan Sun, and Hengde Li, *Preparation and photoluminescence properties of organic-inorganic nanocomposite with a mesolamellar nickel oxide*, **Micropor Mesopor Mat**, **71** (2004) 99.
- [102] M. A. Shah, *A Versatile Route for the Synthesis of Nickel Oxide Nanostructures Without Organics at Low Temperature*, **Nanoscale Res Lett**, **3** (2008) 255.
- [103] F.F. Ferreira, M.H. Tabacniks, M. C. A. Fantini, I. C. Faria, A. Gorenstein, *Electrochromic nickel oxide thin films deposited under different sputtering conditions*, **Solid State Ion**, **86-88** (1996) 971-976.
- [104] F. Saadati, A.-R. Grayeli, H. Savaloni, *Dependence of the optical properties of NiO thin films on film thickness and nano-structure*, **Theor Appl Phy**, **4**(1)(2010) 22-26.
- [105] S. Goldsmith, E. Çetinörgü, R.L. Boxman, *Modeling the optical properties of tin oxide thin films*, **Thin Solid Films**. **517** (2009) 5146
- [106] F. Wooten, *Optical Properties of solids*, Academic, New York, 1981.

- [107] R. A. Smith, *Semiconductors*, Cambridge University Press, Cambridge, 1978.
- [108] J. C. Manifacier, M. De Murcia, I. Fillard, E. Vicario, *Optical and electrical properties of SnO₂ thin films in relation to their stoichiometric deviation and their crystalline structure*, *Thin Solid Films*, **41** (1977) 127.
- [109] S.B. Kulkarni, V.S. Jamadade, D.S. Dhawale, C.D. Lokhande, *Synthesis and characterization of [beta]-Ni(OH)₂ up grown nanoflakes by SILAR method*, *Appl Surf Sci*, **255** (2009) 8390.
- [110] Y. Makimura, A. Rougier, J.-M. Tarascon, *Cobalt and tantalum additions for enhanced electrochromic performances of nickel-based oxide thin films grown by pulsed laser deposition*, *Appl. Surf. Sci*, **252** (13) (2006) 4593-4598.

جامعة النجاح الوطنية
كلية الدراسات العليا

التلوين الكهربائي لأفلام NiO المحضرة بطريقة السول- جل

إعداد

أثير يوسف صالح أبو يعقوب

إشراف

د. إياد سعد الدين

أ.د. حكمت هلال

قدمت هذه الرسالة استكمالاً لمتطلبات الحصول على درجة الماجستير في الفيزياء بكلية الدراسات العليا في جامعة النجاح الوطنية في نابلس، فلسطين.

2012م

ب

التلوين الكهربائي لأفلام NiO المحضرة بطريقة السول - جل

إعداد

اثير يوسف صالح أبو يعقوب

إشراف

د. إياد سعد الدين

أ.د. حكمت هلال

الملخص

تم تحضير أفلام NiO الرقيقة النانوية على شرائح من الزجاج الموصل (FTO/glass) باستخدام مركبات عنصرى التيتانيوم (Ti) والقصدير (Sn) بتركيز مختلفة 5%-30% للعنصر الاول ومن 1%-5%. تم تحضيره الافلام بغمس أحادي وثنائي بطريقة السول جل (الطلاء بالغمس) على شرائح من الزجاج الموصلة عليها مادة (FTO). تم دراسة خصائص عدة لتلك الشرائح بهدف المقارنة بينها منها أطياف الوميض (PL spectra) وسلوكها الكهروكيميائي واقتران الفولتية الدوري وأطياف النفاذية و أشعة اكس و المجهر الالكتروني الماسح. تم دراسة الية التلوين ومورفولوجيا الانتقال للطبقات خلال الدورية في الفولتية وكل ذلك في المحلول الكهرلي 0.5 و 1.0 مولرتي من هيدروكسيد البوتاسيوم وحسبت كذلك كمية الشحنة الداخلة والخارجة من الطبقة خلال عملية التلوين والكثافة البصرية (optical density) وحسبت كذلك فعالية التلوين وفجوة الطاقة وسمك الفلم. كل النتائج تشير الى ان تطعيم مادة اكسيد النيكل بالتيتانيوم والقصدير بتركيز معينة يحسن من الخصائص المختلفة للافلام.